

## The metamorphic evolution of granulites at Fyfe Hills; implications for Archaean crustal thickness in Enderby Land, Antarctica

MICHAEL SANDIFORD, *Department of Geology, University of Melbourne, Parkville 3052, Melbourne, Australia*

**Abstract.** Granulites at Fyfe Hills in Enderby Land, Antarctica, crystallized at temperatures in excess of 850°C, and possibly as high as 1000°C, and at pressures of 8–10 kbar during the mid to late Archaean. A number of features, including repeated retrograde metamorphism at 5.5–8 kbar, retrograde reaction textures, and rimward zoning in pressure sensitive systems, suggest that following peak metamorphism the granulites stabilized at a depth of 18–26 km. After stabilization, the granulites cooled near-isobarically to temperatures of 600–700°C. Assuming a total crustal thickness of 35–40 km during this late Archaean interval of isobaric cooling, the peak metamorphic crustal thickness is estimated at 35–56 km. This estimate is significantly less than the 60–70 km obtained by summing the depths of the present levels of exposure (26–34 km) and the thickness of the crust presently beneath Fyfe Hills (approximately 35 km) and is, therefore, consistent with independent evidence for extensive post-Archaean thickening of the Enderby Land crust.

**Key-words:** Antarctica; Archaean; crustal thickness; geothermobarometry; granulite facies metamorphism

### Abbreviations used in text and figures

cpx	= clinopyroxene
grt	= garnet
hbe	= hornblende
kfs	= K-feldspar
ilm	= ilmenite
mag	= magnetite
mp	= mesoperthite
ol	= olivine
opx	= orthopyroxene
phl	= phlogopite
pig	= pigeonite
pl	= plagioclase
qtz	= quartz
ru	= rutile
sil	= sillimanite

spl	= spinel
spr	= sapphirine
An	= anorthite component
Ab	= albite component
Or	= orthoclase component
Gr	= grossular component
Di	= diopside component
En	= enstatite component
Py	= pyrope component

### INTRODUCTION

Ancient granulite terrains invariably preserve assemblages indicative of crystallization at depths of 25–35 km (Newton & Perkins, 1982). As such, these terrains may either represent the mid-levels of excessively thick continental crust (Condie, 1976; Windley, 1977; Wells, 1981; England & Bickle, 1984), or the base of normal thickness crust (O'Hara, 1977). While there is no general agreement as to which of the two alternative hypotheses is correct, it is in principle possible to discriminate between them by consideration of the pressure-temperature-time (P-T-t) trajectory of a given granulite terrain. This is because temporal variations in P and T in a metamorphic terrain are primarily a function of heat source and the interaction between crustal loading and isostatic response (England & Richardson, 1977; Wells, 1980). A terrain metamorphosed at mid-crustal levels of a thickened crust will be exposed within a few tens to a few hundreds of millions of years after burial, whereas terrains metamorphosed near the base of the crust may, although will not necessarily, remain at deep crustal levels for much longer periods of time.

The granulites at Fyfe Hills and on the adjacent islands in Khmara Bay, in Enderby Land, Antarctica (Fig. 1), contain unusually high grade parageneses such as sapphirine-quartz-mesoperthite. Moreover, they preserve numerous retrograde reaction features (Sandiford & Wilson, 1983, 1984) which allow for the detailed evaluation

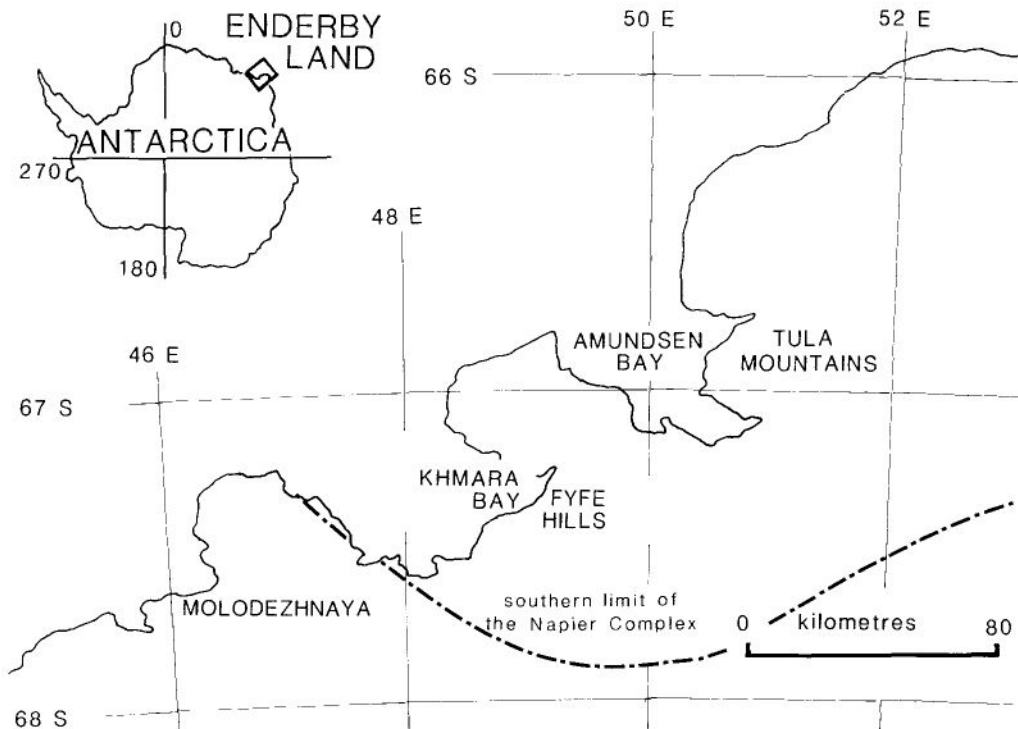


Fig. 1. Geological map of Enderby Land, showing the location of Fyfe Hills and other Antarctic localities described in the text.

of their baric response following the granulite facies event. Constraints on the P-T-t evolution of the Fyfe Hills granulites are considered herein, in order to evaluate the depth relative to total crustal thickness at which they formed.

The Fyfe Hills region occurs near the southwestern margin of the Napier Complex (Fig. 1), an Archaean granulite facies terrain forming one of the oldest segments of the Precambrian shield of East Antarctica (Sheraton, Offe, Tingey & Ellis, 1980; DePaolo, Manton, Grew & Halpern, 1982; Black & James, 1983). The gneissic sequence at Fyfe Hills is composed predominantly of meta-igneous, pyroxene-bearing gneisses ranging in composition from ultrabasic through to acidic, but also includes a variety of gneisses derived from pelitic, ferruginous and calcareous sediments. The oldest gneisses at Fyfe Hills are supracrustal and date back to at least 3.5 Ga (DePaolo *et al.*, 1982) and possibly 3.8 Ga (Compston & Williams, 1982). They were subsequently metamorphosed under granulite facies conditions during the mid to late Archaean (DePaolo *et al.*, 1982; Black, James & Harley, 1983a, 1983b), and suffered various degrees of reworking in the late Proterozoic/early Palaeozoic.

Previous studies (Ellis, 1980; Sheraton *et al.*, 1980; Harley, 1983; Sandiford & Wilson, 1983) have shown that the metamorphic evolution of the Napier Complex involved cooling from unusually high peak metamorphic temperatures which occurred at nearly constant pressure. This type of metamorphism differs significantly from the type of metamorphism in the metamorphic terrains of the Phanerozoic foldbelts, and raises queries about the processes of crustal formation in the Archaean. The evaluation of synmetamorphic crustal thickness is essential to the elucidation of such processes, and is the main theme of this contribution.

#### SEQUENCE OF METAMORPHIC CRYSTALLIZATION AT FYFE HILLS

The sequence of metamorphic crystallization used as a basis to distinguish metamorphic events in this contribution (Table 1) stems from the structural and microstructural analysis of timing relationships described in Sandiford & Wilson (1984) which is briefly summarized here. The tectonic evolution of the Fyfe Hills region involves five deformation events ( $D_1$ - $D_5$ ), associated with

**Table 1.** Correlation of metamorphic events at Fyfe Hills with structural chronology (Sandiford & Wilson, 1984)

Metamorphic event	Deformation event	Intrusive rocks	Age (Ga)	Pressure (kbar)	Temperature (°C)
M <sub>1</sub>	D <sub>1</sub>		3.1*-2.5†	7.8-10.0	850-1000
M <sub>2</sub>	D <sub>2</sub>		2.5‡-2.35§	5.5-7.5	590-690
M <sub>3</sub>	D <sub>3</sub>	Khmara dyke	1.4-1.0§	4.5-8.5	
M <sub>4</sub>	D <sub>4</sub> (RSZ)	Amundsen dyke	1.0-0.5‡	5.5-8.0	620-720
M <sub>4</sub>	D <sub>5</sub> (RSZ)	RSZ pegmatites	1.0-0.5‡	4.5-7.0	600-700
			0.5‡	3.0-5.0	600-650

Metamorphic data for late Proterozoic RSZ events taken from Sandiford (1985).

\* Black *et al.* (1983a).

† DePaolo *et al.* (1982).

‡ Black *et al.* (1983b).

§ Sheraton & Black (1981).

four chronologically distinct syntectonic metamorphic events. These include (1) a highest grade, granulite event (M<sub>1</sub>) broadly coeval with D<sub>1</sub> and D<sub>2</sub>, and which has been variously dated at 3.1 Ga (Black *et al.*, 1983a) and 2.5 Ga (DePaolo *et al.*, 1982); (2) a retrograde granulite facies event (M<sub>2</sub>) coeval with D<sub>3</sub> between 2.5 Ga (Black *et al.*, 1983b) and 2.35 Ga, the latter being the age of a suite of unmetamorphosed dykes in the Napier Complex (Sheraton & Black, 1981); (3) a retrograde amphibolite facies event (M<sub>3</sub>) associated with the formation of D<sub>4</sub> retrograde shear zones (RSZs) after the intrusion of the Amundsen dykes (Sheraton & Black, 1981); and (4) retrograde amphibolite facies metamorphism (M<sub>4</sub>) associated with the formation of mylonite zones and intrusion of 500 Ma-old pegmatites (Black *et al.*, 1983b; Sandiford, 1985).

The age of the RSZs are poorly constrained (Sandiford & Wilson, 1984). They may have been initiated during the 1000 Ma 'Rayner' metamorphism (Black *et al.*, 1983b), when extensive reworking of the Precambrian crust occurred in crystalline blocks adjacent to the Napier Complex (Grew, 1978). Alternatively, the RSZs may represent the initial stages of the 500 Ma retrogression associated with the intrusion of pegmatites. Whichever the case, the retrogression represents reworking of the Fyfe Hills granulites after prolonged tectonic quiescence, which apparently lasted throughout the early and mid Proterozoic (Sandiford & Wilson, 1984).

#### ANALYTICAL TECHNIQUES

Mineral analyses (Tables 2-5) have been performed on the Melbourne University Jeol JXA-5A electron microprobe operating with an accelerating voltage of 15 kV and a beam width

of 10-15 µm. The data were reduced according to Ferguson & Sewell (1980). Samples numbers prefixed by R are Melbourne University Geology Department Museum numbers. Each of the mineral compositions presented in Tables 2-5 is the average of three or more individual analyses from different areas of the one grain. Minerals have been accepted for thermometric calculations only when the variations of individual analyses are within the bounds of the microprobe analytical error (approximately ±2% for major elements).

#### GRANULITE FACIES METAMORPHISM AT FYFE HILLS

The M<sub>1</sub> assemblages are defined by coarse-grained granoblastic microstructures associated with D<sub>1</sub> and D<sub>2</sub> structures and are the highest grade mineral assemblages observed at Fyfe Hills. They are characteristic of the pyroxene-granulite facies (Table 6). The M<sub>2</sub> hornblende-granulite facies assemblages are characterized by fine- to medium-grained, equigranular, granoblastic microstructures associated with D<sub>3</sub> tectonite fabrics. They have been observed in a number of mafic and felsic meta-igneous gneisses and in a suite of metamorphosed mafic dykes termed the Khmara dykes (R25387 and R25856), which were intruded during D<sub>3</sub>, as well as in phlogopite-rich zones in metapelites on McIntyre Island.

#### M<sub>1</sub> assemblages in meta-igneous gneisses

Typical M<sub>1</sub> assemblages in felsic meta-igneous gneisses are mesoperthite (or antiperthite) orthopyroxene-quartz-ilmenite (Fig. 2a); while intermediate and basic meta-igneous gneisses contain orthopyroxene-clinopyroxene assemblages. Garnet is absent from M<sub>1</sub> meta-igneous clinopyroxene-bearing assemblages (including both quartz-absent and quartz-bearing gneisses of

**Table 2.** Composition of orthopyroxene determined by electron microprobe

Sample	Analysis																							
	1	2	3	4	5	6	7	8	9	10	11	12	13	14	15	16	17	18	19	20	21	22	23	
	R25402	R253848	R25544	R25620		R25662		R25800		R31038		R31096	R31126	R31128	R31130		R31134		R25387	R25402	R25404	R25680	R25856	
	Core	Core	Core	Core	Rim	Core	Rim	Core	Rim	Core	Rim	Core	Core	Core	Core	Rim	Core	Rim	Core	Core	Core	Core	Core	Core
SiO <sub>2</sub>	51.20	49.88	56.49	61.69	51.62	52.05	52.44	47.44	50.55	50.37	51.01	50.45	55.32	54.32	48.89	50.20	51.68	54.29	50.75	50.85	50.79	50.14	50.58	
TiO <sub>2</sub>	0.08	1.10	—	0.04	0.06	0.09	0.11	0.12	0.07	0.08	0.07	0.05	0.06	0.17	0.09	0.62	—	0.07	0.04	—	—	0.12	0.09	
Al <sub>2</sub> O <sub>3</sub>	1.32	0.76	1.54	1.91	1.73	6.02	5.29	10.48	5.28	1.22	1.10	1.39	2.30	4.37	1.96	1.63	1.79	2.44	0.97	1.03	2.11	1.10	0.97	
FeO	10.32	34.28	10.32	25.91	25.99	16.45	16.71	19.76	20.26	29.72	29.56	9.77	28.86	9.41	28.86	28.56	14.89	14.96	31.79	27.54	27.08	29.99	31.65	
MnO	0.44	0.34	0.18	0.16	0.17	0.11	0.09	0.09	0.09	0.16	0.14	0.55	0.03	0.20	0.56	0.63	0.34	0.30	0.44	0.47	0.29	0.40	0.35	
MgO	18.88	13.96	31.76	2.55	20.64	25.73	26.15	21.87	24.19	17.40	17.84	18.69	31.24	31.29	17.52	17.63	28.09	27.15	16.51	18.33	19.13	17.57	16.14	
CaO	0.50	0.68	0.33	0.23	0.18	0.03	0.03	0.09	0.11	0.52	0.49	0.88	0.27	0.25	0.54	0.54	0.39	0.44	0.45	0.35	0.45	0.43	0.57	
Na <sub>2</sub> O	—	—	—	—	—	0.04	—	—	—	—	—	0.18	0.06	0.02	—	—	—	—	—	—	—	—	—	
Cr <sub>2</sub> O <sub>3</sub>	—	—	0.25	—	—	tr	—	0.06	0.02	—	—	tr	0.64	0.18	—	—	0.05	0.05	—	—	—	—	—	
Total	99.46	99.10	100.87	100.49	99.99	100.52	100.82	98.91	100.57	99.47	100.21	99.92	99.96	100.21	99.40	99.21	100.23	99.70	100.95	99.12	99.85	99.75	100.35	
Si	1.962	1.963	1.965	1.944	1.949	1.868	1.879	1.731	1.852	1.956	1.956	1.940	1.942	1.897	1.935	1.948	1.957	1.953	1.960	1.962	1.939	1.947	1.965	
Al <sup>IV</sup>	0.038	0.036	0.035	0.056	0.051	0.132	0.121	0.269	0.148	0.044	0.038	0.060	0.058	0.103	0.065	0.052	0.043	0.047	0.040	0.038	0.061	0.050	0.035	
Al <sup>VI</sup>	0.022	—	0.028	0.029	0.026	0.123	0.103	0.192	0.090	0.012	0.012	0.003	0.037	0.077	0.025	0.023	0.033	0.056	0.004	0.009	0.034	—	0.009	
Ti	0.002	0.003	—	0.001	0.006	0.002	0.003	0.003	0.002	0.002	0.002	0.001	0.002	0.004	0.003	0.001	—	0.001	0.001	—	—	0.004	0.003	
Fe <sup>2+</sup>	0.865	1.147	0.300	0.815	0.808	0.494	0.501	0.616	0.621	0.965	0.951	0.892	0.287	0.275	0.963	0.927	0.446	0.450	1.027	0.889	0.864	0.974	1.028	
Mn	0.014	0.012	0.005	0.005	0.005	0.003	0.003	0.003	0.003	0.005	0.005	0.018	0.009	0.006	0.018	0.021	0.010	0.009	0.014	0.015	0.009	0.013	0.012	
Mg	1.079	0.833	1.647	1.152	1.162	1.377	1.397	1.215	1.321	1.007	1.023	1.071	1.635	1.629	1.013	1.020	1.499	1.456	0.951	1.086	1.088	1.017	0.935	
Ca	0.023	0.029	0.012	0.009	0.007	0.001	0.001	0.004	0.040	0.022	0.020	0.036	0.010	0.009	0.022	0.022	0.615	0.017	0.019	0.014	0.018	0.018	0.024	
Na	—	—	—	—	—	0.003	—	0.004	—	—	—	0.013	0.004	0.001	—	—	—	—	—	—	—	—	—	
Cr	—	—	0.007	—	—	—	—	—	—	—	—	—	0.018	0.005	—	—	0.001	0.001	—	—	—	—	—	
Total	4.005	4.019	4.000	4.012	4.011	4.003	4.006	4.037	4.033	4.014	4.011	4.034	4.002	4.007	4.017	4.014	4.004	4.992	4.016	4.014	4.014	4.023	4.010	

Structural formula calculated on the basis of 6 oxygens. Analyses 1–18 are from M<sub>1</sub> assemblages. Analyses 19–23 are from M<sub>2</sub> assemblages.

**Table 3.** Composition of clinopyroxene determined by electron microprobe

Sample	Analysis													
	1 R25384B	2 R25402	3 R25544	4 R31038	5 R31096	6 R31130	7 R31134	8 R25387	9 R25402	10 R25404	11 R25680	12 R25856	13	14
	Core	Core	Core	Core	Core	Core	Rim	Core	Rim	Core	Core	Core	Core	Core
SiO <sub>2</sub>	50.01	51.10	52.80	50.44	49.95	49.78	49.78	52.41	52.50	51.30	51.13	49.73	50.36	50.96
TiO <sub>2</sub>	0.29	0.25	—	0.28	0.29	0.46	0.38	0.36	0.26	0.20	0.28	0.31	0.28	0.22
Al <sub>2</sub> O <sub>3</sub>	1.93	2.19	2.97	2.63	3.20	3.32	3.62	3.25	3.32	2.17	2.22	3.70	2.80	2.19
FeO	14.46	10.82	2.73	11.44	10.44	12.57	11.40	4.67	4.44	11.82	9.86	9.80	11.85	12.58
MnO	0.17	0.19	0.09	0.05	0.24	0.27	0.24	0.17	0.16	0.20	0.19	0.10	0.20	0.15
MgO	9.93	12.32	15.49	11.67	11.99	11.66	11.07	15.06	15.53	11.74	12.63	12.01	11.66	11.20
CaO	20.96	21.35	23.20	21.79	21.67	20.21	21.61	22.90	23.53	21.61	22.39	22.18	21.45	21.88
Na <sub>2</sub> O	0.60	0.50	0.60	0.62	0.59	0.67	0.69	0.53	0.42	0.55	0.47	0.68	0.66	0.61
Cr <sub>2</sub> O <sub>3</sub>	—	—	0.94	—	0.07	—	—	0.11	0.11	—	—	—	—	—
Total	98.35	99.02	98.82	98.92	98.44	98.94	98.79	99.46	100.07	99.59	99.17	98.51	99.26	99.79
Si	1.949	1.943	1.945	1.929	1.913	1.908	1.907	1.932	1.924	1.948	1.938	1.900	1.922	1.941
Al <sup>IV</sup>	0.051	0.057	0.055	0.071	0.087	0.092	0.093	0.068	0.076	0.052	0.062	0.100	0.078	0.059
Al <sup>V</sup>	0.037	0.041	0.064	0.048	0.057	0.058	0.070	0.078	0.067	0.045	0.037	0.067	0.048	0.039
Ti	0.009	0.007	—	0.008	0.008	0.013	0.011	0.010	0.007	0.006	0.008	0.009	0.008	0.006
Fe <sup>2+</sup>	0.471	0.344	0.084	0.366	0.334	0.403	0.365	0.144	0.137	0.375	0.313	0.313	0.378	0.401
Mn	0.006	0.006	0.003	0.002	0.008	0.009	0.008	0.005	0.005	0.006	0.006	0.003	0.007	0.005
Mg	0.577	0.715	0.851	0.665	0.684	0.666	0.632	0.827	0.837	0.665	0.714	0.684	0.663	0.636
Ca	0.875	0.870	0.916	0.893	0.889	0.830	0.887	0.904	0.924	0.879	0.909	0.908	0.873	0.893
Na	0.045	0.037	0.043	0.046	0.044	0.050	0.051	0.038	0.030	0.041	0.035	0.050	0.049	0.045
Cr	—	0.027	—	—	—	—	—	0.003	0.003	—	—	—	—	—
Total	4.021	4.020	3.998	4.027	4.028	4.029	4.026	4.005	4.011	4.018	4.022	4.033	4.026	4.026

Structural formula calculated on the basis of 6 oxygens. Analyses 1–9 are from M<sub>1</sub> assemblages. Analyses 10–14 are from M<sub>2</sub> assemblages.

**Table 4.** Composition of garnet determined by electron microprobe

Sample	Analysis																				9		10		11		12		13		14		15		16		17		18		19		20		
	R25384			R25620			R25631			R25660			R25662			R25800			R25824			R31038			R31130			R25387			R25405			R25686			R25856			R25624					
	Corona	Core	Rim	Corona	Core	Rim	Corona	Core	Rim	Corona	Core	Rim	Corona	Core	Rim	Corona	Core	Rim	Corona	Core	Core	Core	Core	Core	Core	Core	Core	Core	Core	Core	Core	Core	Core	Core	Core	Core	Core	Core	Core	Core					
SiO <sub>2</sub>	37.49	38.94	38.70	41.03	40.64	41.12	40.30	40.59	38.48	39.41	39.11	39.31	38.01	37.90	37.84	37.80	37.39	37.85	40.35	40.48																									
TiO <sub>2</sub>	0.09	0.06	0.02	—	—	—	0.02	0.05	0.11	0.05	0.06	—	0.07	0.08	0.06	0.06	0.03	—	0.07	—	—	—	—	—	—	—	—	—	—	—	—	—	—	—	—	—	—	—	—	—					
Al <sub>2</sub> O <sub>3</sub>	20.56	21.43	21.57	23.47	22.92	23.24	22.77	22.59	22.40	23.07	22.46	22.68	20.99	20.45	21.23	21.27	20.70	20.78	22.81	22.57																									
FeO	30.10	29.56	29.92	18.76	19.00	19.76	23.19	23.26	26.15	22.81	24.05	24.40	28.85	27.51	30.09	28.45	29.44	29.81	22.11	23.13																									
MnO	1.10	0.41	0.39	0.15	0.18	0.08	0.20	0.14	0.26	0.32	0.28	0.27	0.38	1.27	1.05	0.85	1.18	1.05	0.16	0.16																									
MgO	2.74	7.42	6.99	16.66	15.63	16.34	14.07	13.67	11.10	11.49	11.95	11.62	4.73	5.37	3.69	5.01	3.88	3.79	15.10	14.34																									
CaO	7.16	3.39	3.65	1.08	1.56	0.62	0.68	0.68	1.42	0.86	1.62	1.78	7.05	6.95	6.90	6.89	7.27	7.14	0.27	0.25																									
Na <sub>2</sub> O	—	—	—	—	—	—	—	—	—	—	—	—	—	—	—	—	—	—	—	—	—	—	—	—	—	—	—	—	—	—	—	—	—	—	—	—	—								
Cr <sub>2</sub> O <sub>3</sub>	—	—	—	—	—	—	—	—	—	—	—	—	—	—	—	—	—	—	—	—	—	—	—	—	—	—	—	—	—	—	—	—	—	—	—	—	—								
Total	99.24	101.21	101.14	101.16	99.93	101.27	100.23	100.98	100.00	101.91	99.63	100.06	100.08	99.33	100.86	100.33	98.89	100.42	100.87	100.01																									
Si	3.017	3.018	2.993	2.977	2.995	2.989	2.982	3.009	2.942	2.949	2.970	2.975	2.995	3.000	2.982	2.971	2.978	2.997	2.971	2.996																									
Ti	0.005	0.004	0.001	—	—	—	0.001	0.003	0.006	0.003	0.003	—	0.004	0.005	0.004	0.004	0.002	—	—	—	—																								
Al	1.950	1.923	1.966	2.007	1.999	1.992	1.986	1.974	2.018	2.035	2.010	2.025	1.949	1.908	1.972	1.971	1.944	1.939	1.985	1.969																									
Fe <sup>2+</sup>	2.026	1.913	1.929	1.138	1.171	1.202	1.435	1.442	1.672	1.665	1.527	1.544	1.901	1.828	1.983	1.870	1.962	1.974	1.365	1.432																									
Mn	0.069	0.027	0.026	0.010	0.11	0.005	0.013	0.009	0.017	0.020	0.018	0.017	0.025	0.085	0.070	0.057	0.040	0.070	0.010	0.010																									
Mg	0.329	0.857	0.806	1.802	1.717	1.771	1.552	1.511	1.265	1.282	1.353	1.311	0.556	0.634	0.434	0.587	0.460	0.447	1.662	1.582																									
Ca	0.617	0.277	0.302	0.084	0.123	0.048	0.054	0.054	0.116	0.069	0.832	0.144	0.595	0.589	0.583	0.580	0.620	0.606	0.021	0.020																									
Na	—	—	—	—	—	—	—	—	0.012	0.015	—	—	—	—	—	—	—	—	—	—																									
Cr	—	—	—	—	—	—	0.005	—	—	—	—	—	—	—	—	—	—	—	—	—																									
Total	8.013	8.018	8.023	8.019	8.009	8.012	8.023	8.003	8.049	8.038	8.019	8.015	8.026	8.042	8.028	8.040	8.006	8.034	8.025	8.014																									

Structural formula calculated on the basis of 12 oxygens. Analyses 1–14 are from M<sub>1</sub> assemblages. Analyses 15–20 are from M<sub>2</sub> assemblages.

**Table 5.** Composition of plagioclase determined by electron microprobe

Sample	Analysis																								
	R25384B			R25620		R25631		R25660		R25662		R25800		R25824		R31038		R31130	R25387	R25403	R25404	R25405	R25686	R25856	R25624
	Core	Core	Rim	Core	Rim	Core	Core	Rim	Core	Rim	Core	Rim	Core	Rim	Core										
SiO <sub>2</sub>	59.31	60.54	57.80	59.51	57.73	62.74	64.08	64.62	60.78	59.63	57.60	57.70	53.39	57.01	55.55	58.60	52.85	57.04	55.18	57.94	59.47	66.56			
Al <sub>2</sub> O <sub>3</sub>	24.38	24.45	25.70	24.43	25.60	22.43	22.33	21.89	24.41	25.36	26.33	26.52	28.17	26.35	26.90	25.56	28.61	26.72	27.82	25.56	24.87	20.20			
Fe <sub>2</sub> O <sub>3</sub>	0.10	0.09	0.11	0.06	0.16	0.04	—	0.20	0.27	0.67	0.05	0.27	0.19	0.35	0.31	0.01	0.10	0.16	0.16	0.16	0.14	0.02			
CaO	6.55	6.65	7.79	7.08	7.24	4.17	3.84	3.43	5.84	6.57	8.44	8.45	11.18	8.79	0.65	7.42	11.65	9.20	10.04	7.91	7.03	1.73			
Na <sub>2</sub> O	7.77	7.82	7.03	7.73	7.38	9.33	9.58	9.85	8.46	7.84	6.95	6.75	5.10	6.38	6.09	7.11	4.85	6.44	5.84	6.89	7.47	10.59			
K <sub>2</sub> O	0.30	0.36	0.13	0.17	0.19	0.08	0.15	0.13	0.06	0.01	0.06	0.09	0.10	0.20	0.38	0.19	0.27	0.17	0.29	0.33	0.40				
Total	98.41	99.91	98.56	99.98	98.30	98.80	99.98	100.12	99.81	100.09	99.43	99.79	98.13	99.08	98.73	99.17	98.24	99.82	99.21	98.75	99.51	99.50			
Si	10.750	10.801	10.484	10.624	10.511	11.228	11.322	11.393	10.834	16.630	10.376	10.351	9.834	10.328	10.248	10.558	9.736	10.268	10.021	10.498	10.663	11.753			
Al	5.209	5.142	5.495	5.351	5.475	4.729	4.634	4.549	5.129	5.329	5.591	5.608	6.116	5.627	5.793	5.428	6.213	5.669	5.954	5.498	5.282	4.204			
Fe <sup>3+</sup>	0.015	0.013	0.017	0.009	0.024	0.006	—	0.029	0.036	0.090	0.008	0.041	0.029	0.053	0.047	0.015	0.021	0.024	0.024	0.024	0.024	0.003			
Ca	1.272	1.271	1.514	1.354	1.408	0.799	0.728	0.648	1.116	1.254	1.629	1.624	2.207	1.706	1.887	1.422	2.300	1.774	1.954	1.536	1.354	0.327			
Na	2.731	2.705	2.472	2.676	2.601	3.235	3.285	3.367	2.925	2.710	2.428	2.351	1.821	2.241	2.155	2.484	1.732	2.248	2.055	2.421	2.602	3.626			
K	0.069	0.082	0.030	0.039	0.040	0.018	0.029	0.029	0.013	0.003	0.014	0.021	0.023	0.046	0.047	0.087	0.046	0.068	0.040	0.667	0.097	0.090			
Total	20.046	20.015	20.012	20.053	20.059	20.009	20.008	19.998	20.053	20.016	20.045	20.003	20.031	20.002	20.067	20.006	20.040	20.042	20.049	20.004	20.008	20.003			

Structural formula calculated on the basis of 32 oxygens. Analyses 1–15 are from M<sub>1</sub> assemblages. Analyses 16–22 are from M<sub>2</sub> assemblages.

**Table 6.** Diagnostic granulite assemblages for the principal rock types in the Fyfe Hills region

Rock type	$M_1$ assemblages	$M_2$ assemblages
Meta-igneous gneisses	opx-cpx mp qtz ilm opx cpx pl-qtz-ilm mag opx ol-Ti hbe spl (phl)	opx cpx-hbe grt-kfs-pl-qtz-ilm
Meta-pelitic gneisses	spr grt qtz-pl-ru spr qtz mp-opx-ru sil-opx-mp-qtz ru sil grt-pl-qtz ru opx grt-pl qtz ru	grt phl-sil pl-kfs qtz
Fe-rich metasediments	sub Ca cpx-pig mag qtz opx pig-mag-qtz	

tholeiitic composition). Ti-hornblende (with the composition:  $(K_{0.34}Na_{0.64})(Cr_{0.07}Ca_{1.85}Mg_{3.11}Fe_{0.92}Ti_{4.6}Al_{0.39})(Al_{1.97}Si_{6.03})O_{23}$ , which closely approaches kaersutite) occurs in ultramafic gneisses along with olivine, spinel, and orthopyroxene, and is the only hydrate for which there is unequivocal evidence of  $M_1$  microstructural equilibrium (Fig. 2b).

Temperatures based on  $M_1$  clinopyroxene-orthopyroxene compositions are shown in Table 7. Pyroxenes in these assemblages invariably exhibit some exsolution features (Sandiford & Powell, unpublished data) and while no attempt has been made to integrate lamellae compositions only those pyroxene with less than a few modal % lamellae have been used in these calculations. Wells' (1977) pyroxene-solvus thermometer yields

temperatures in the range 783–917°C (average 865°C) for  $M_1$  assemblages (Table 7). The pronounced inverse correlation between the Wells temperatures and the mg number ( $mg = Mg/Mg + Fe$ ) of the coexisting pyroxenes implies that this thermometer is of little value in constraining metamorphic temperatures at Fyfe Hills (see also Harley, 1981). Moreover, as all  $M_1$  clinopyroxene-orthopyroxene pairs contain mutual exsolution lamellae, the pyroxene-solvus temperatures must be considered minima. This is supported by evidence, based on pyroxene exsolution in Fe-rich metasediments at Fyfe Hills, that metamorphic temperatures exceeded 1000°C (Sandiford & Powell, unpublished data), and indicates that pyroxene-solvus chemistry has failed to preserve peak conditions at Fyfe Hills (see below).

**Table 7.** Geothermometry of granulite assemblages Fyfe Hills

Event	Sample	$a_{En,opx}$	$a_{Di,opx}$	$X_{Fe,opx}$	$Fe/Mg_{opx}$	$X_{Fe,grt}$	$\ln K^a$	$\ln K^b$	$\ln K^c$	Temperature (°C)				
										$T_1$	$T_2$	$T_3$	$T_4$	$T_5$
$M_1$	R25402	0.290	0.423	0.424			-1.926			851	889			
	R25544	0.678	0.277	0.150			-3.196			879	788			
	R31096	0.282	0.029	0.392			-2.288			825	839			
	R31126	0.667	0.026	0.140			-3.025			879	783			
	R31130	0.255	0.047	0.465			-1.677			861	917			
	R31134	0.561	0.037	0.217			-2.697			890	843			
corona	R25384B	0.172	0.024	0.542	0.219	0.664	-1.965	2.217	1.532	792	832	746	637	644
	R31038	0.260	0.028	0.458	0.154	0.608	-2.211	2.036	1.296	801	825	777	674	731
	R31130	0.258	0.025	0.441	0.149	0.564	-2.334	1.902	1.129	793	810	811	706	805
$M_2$	R25387	0.224	0.032	0.488	0.360	0.631	-1.955	2.247	1.447	817	856	737	624	663
	R25402	0.292	0.027	0.422			-2.367			800	814			
	R25405	0.294	0.023	0.409	0.116	0.587	-2.530	2.267	1.372	788	793	732	620	703
	R25686	0.256	0.032	0.450	0.155	0.610	-2.074	2.221	1.558	820	852	747	639	632
	R25856	0.217	0.024	0.498	0.174	0.661	-2.190	2.216	1.367	785	813	756	649	695

$K^a = a_{Di,opx}/a_{En,opx}$ ;  $K^b = (Fe/Mg)_{grt}/(Fe/Mg)_{opx}$ ;  $K^c = (Fe/Mg)_{grt}/(Fe/Mg)_{opx}$ . Temperature estimates after: Wood & Banno (1973),  $T_1$ ; Wells (1977),  $T_2$ ; Ganguly (1979),  $T_3$ ; Ellis & Green (1979),  $T_4$ ; Harley (1981),  $T_5$ . Mineral analyses tabulated in Tables 2–4.

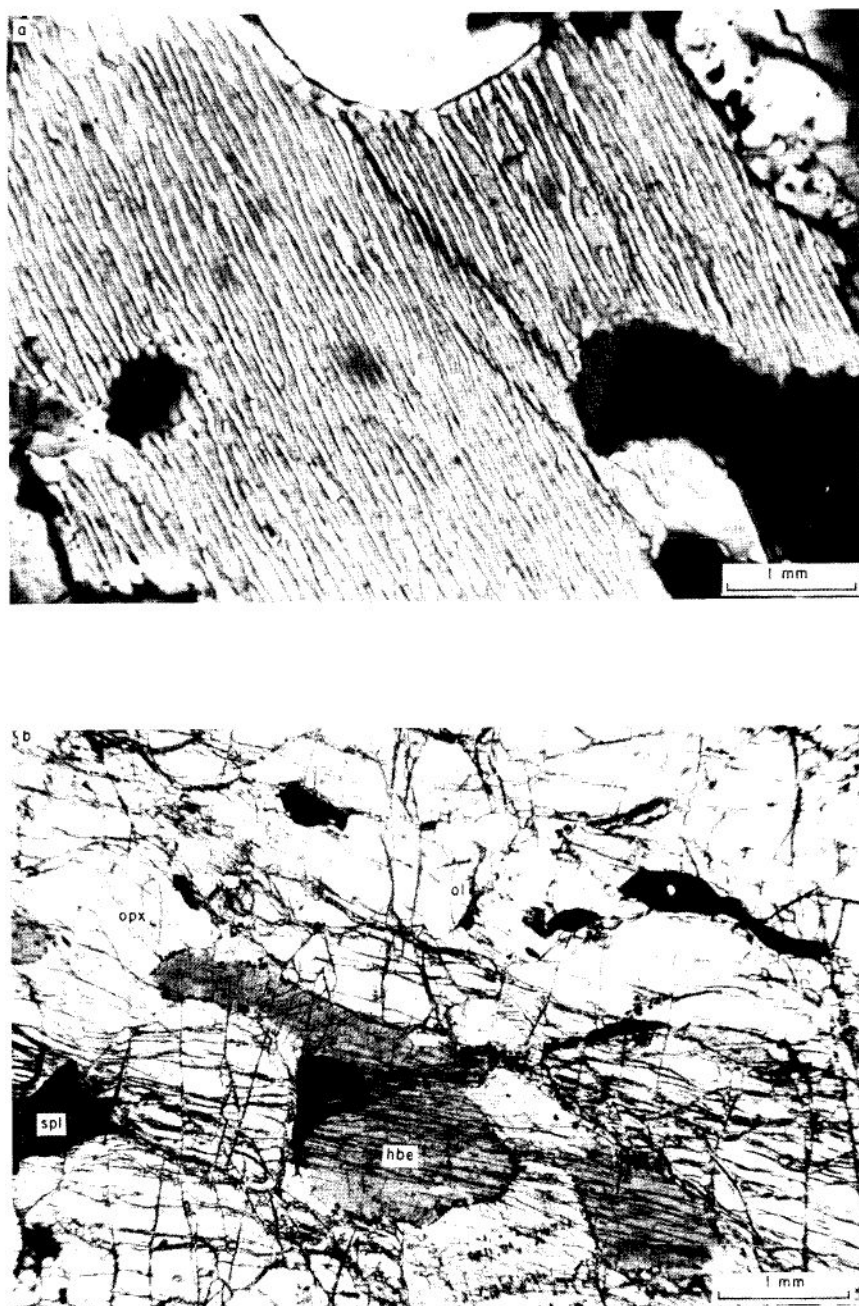
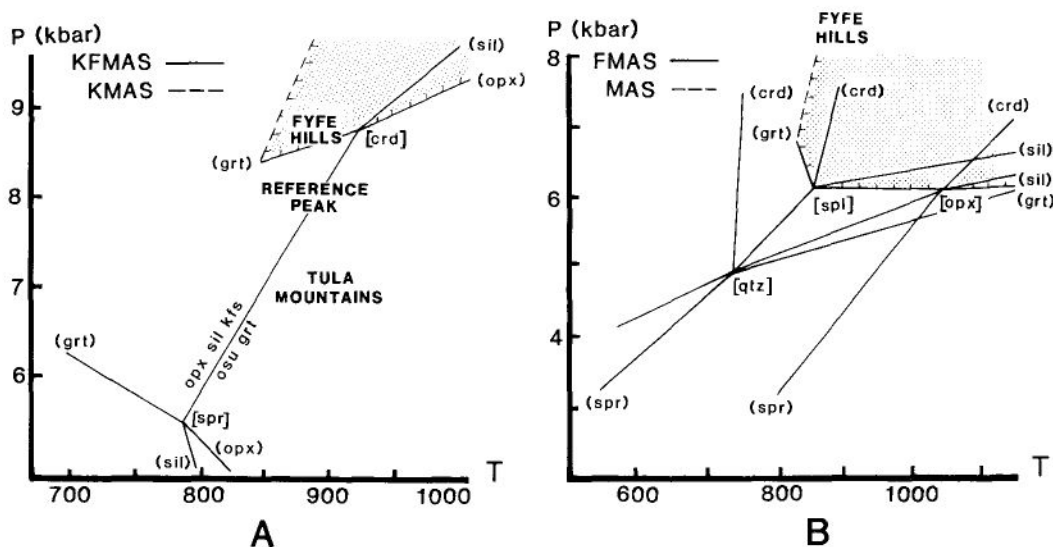
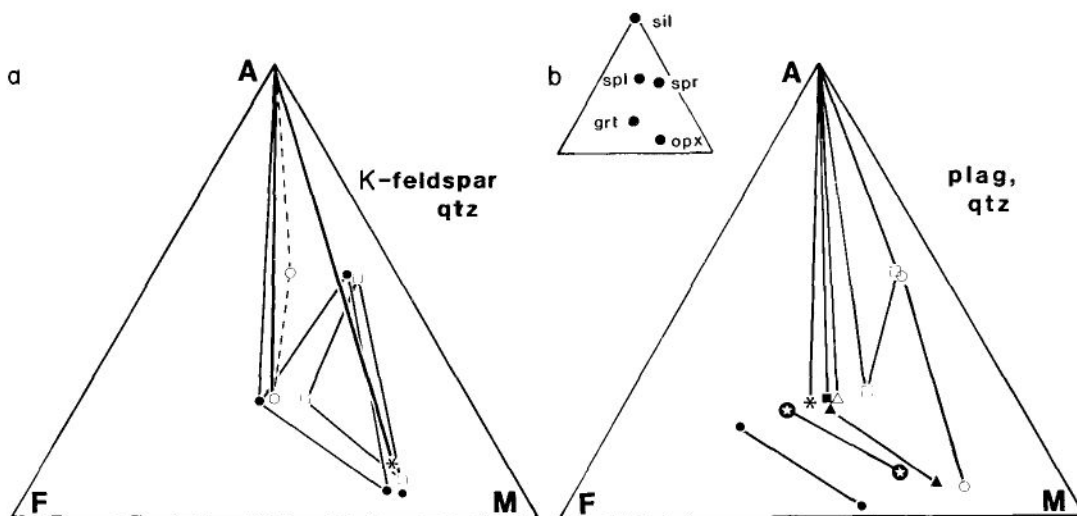


Fig. 2a. Mesoperthite ( $\text{Ab}_{44}\text{An}_{10}\text{Or}_{46}$ ) in charnockitic gneiss (R25579). 2b. Hornblende (hbe)-olivine (ol)-orthopyroxene (opx) spinel (spl) assemblage in ultrabasic gneiss (R25399).



**Fig. 3a.** Petrogenetic grid for KFMAS, based on assemblages recorded from the Tula Mountains (after Grew, 1982a; see also Ellis *et al.*, 1980). Univariant reactions marked by absent phases in parentheses, invariant points marked by absent phase in square brackets. The stability field of sapphirine-K-feldspar-quartz is shaded. P coordinates are based on pressure-assemblage variations in the Napier Complex (see also Grew, 1982a). **3b.** Petrogenetic grid for FMAS based on assemblages developed in the Napier Complex and Southern India (after Grew, 1982b). Bracketing as for Fig. 3a. The stability field of sapphirine-quartz is shaded.



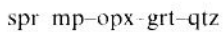
**Fig. 4.** AFM projections for metapelites R25628 (solid circle), R25641 (open circle), R25656 (square), R25657 (triangle) with mesoperthite and quartz (projected from K-feldspar). **4b.** AFM projections for metapelites R25533 (open circle), R25620 (solid circle), R25631 (open square), R25650 (solid square), R25660 (open triangle), R25662 (solid triangle), R25800 (open star), R25824 (solid star) with plagioclase and quartz (projected from anorthite).

**M<sub>1</sub> assemblages in metapelites**

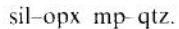
Ellis, Sheraton, England & Dallwitz (1980) and Grew (1982a) have shown that assemblages in metapelites in the Napier Complex are sensitive to relatively small changes in P and T as well as in bulk composition, and thus provide a basis for discriminating regional P-T variations in the Napier Complex. Previous studies of metapelitic assemblages in the Napier Complex have been largely restricted to the Tula Mountains (Fig. 1) where granulite facies P and T have been estimated as 8–10 kbar and 900–980°C (Ellis, 1980; Ellis *et al.*, 1980) and 6–8 kbar and 870–930°C (Grew, 1980). The diagnostic metapelitic assemblages in the Tula Mountains are sapphirine-quartz (in systems approaching FMAS) and osumilite-quartz (KFMAS) (Ellis *et al.*, 1980; Grew, 1980, 1982a). The osumilite-bearing parageneses are particularly important because they have been recorded from only a few granulite terrains (see Grew, 1982a) and are indicative of temperatures rarely attained during crustal metamorphism (Fig. 3a).

The M<sub>1</sub> chemographic relations in Fyfe Hills metapelites are illustrated in Fig. 4. In systems which approximate FMAS, the typical assemblage is sapphirine-quartz. Osumilite has not been recorded. The following assemblages occur

in systems approximating KFMAS (Figs 5, 6a):



and



The spinel-quartz (Fig. 6b) assemblage is stabilized with respect to lower temperature, equivalent, sapphirine- and orthopyroxene-bearing assemblages by Zn (gahnite forms 22 mol. % of the spinel in Fig. 6b). Sillimanite-orthopyroxene-quartz assemblages are difficult to reconcile with the more common assemblage sapphirine-quartz-garnet as they suggest that both the sapphirine garnet and sillimanite-orthopyroxene tielines were operative (Fig. 4a). However, the small grossular contents in garnet (up to 3 mol. %) coexisting with sapphirine suggest that the garnet-sapphirine assemblage is not strictly stable in FMAS or KFMAS. Therefore, the Fyfe Hills metapelites most likely crystallized in the divariant (in FMAS) sillimanite sapphirine-orthopyroxene-quartz stability field (Fig. 3b).

The absence of osumilite in the Fyfe Hills region may be due to the stability of the similar assemblages orthopyroxene sillimanite mesoperthite quartz and sapphirine orthopyroxene-mesoperthite-quartz. These assemblages have not been reported from other parts of

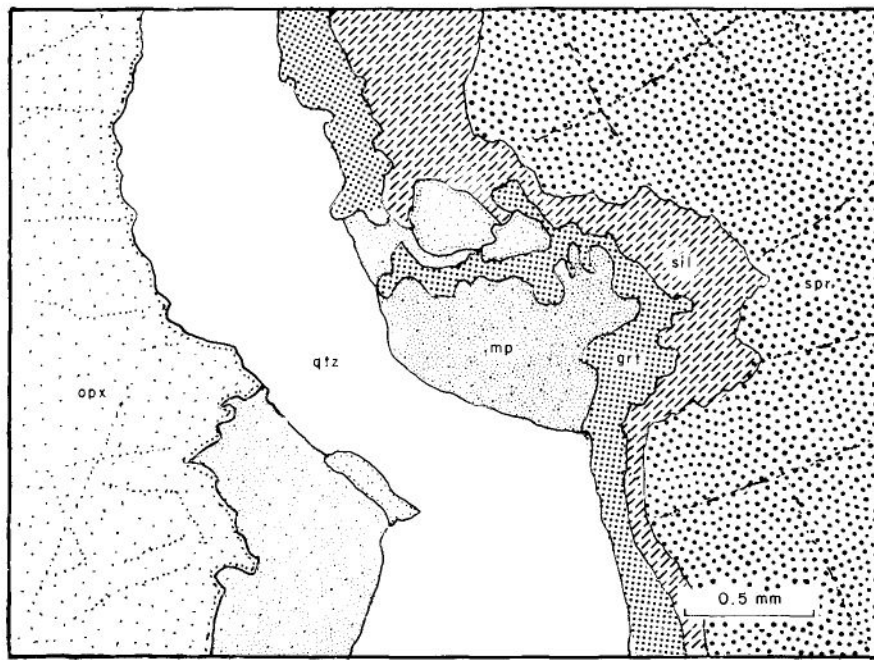


**Fig. 5.** M<sub>1</sub> opx-spr-qtz-mp assemblage in metapelite R25628. Orthopyroxene contains very fine plagioclase exsolution lamellae and is partially replaced by phlogopite. Mesoperthite and sapphirine are separated by a sillimanite-garnet corona.

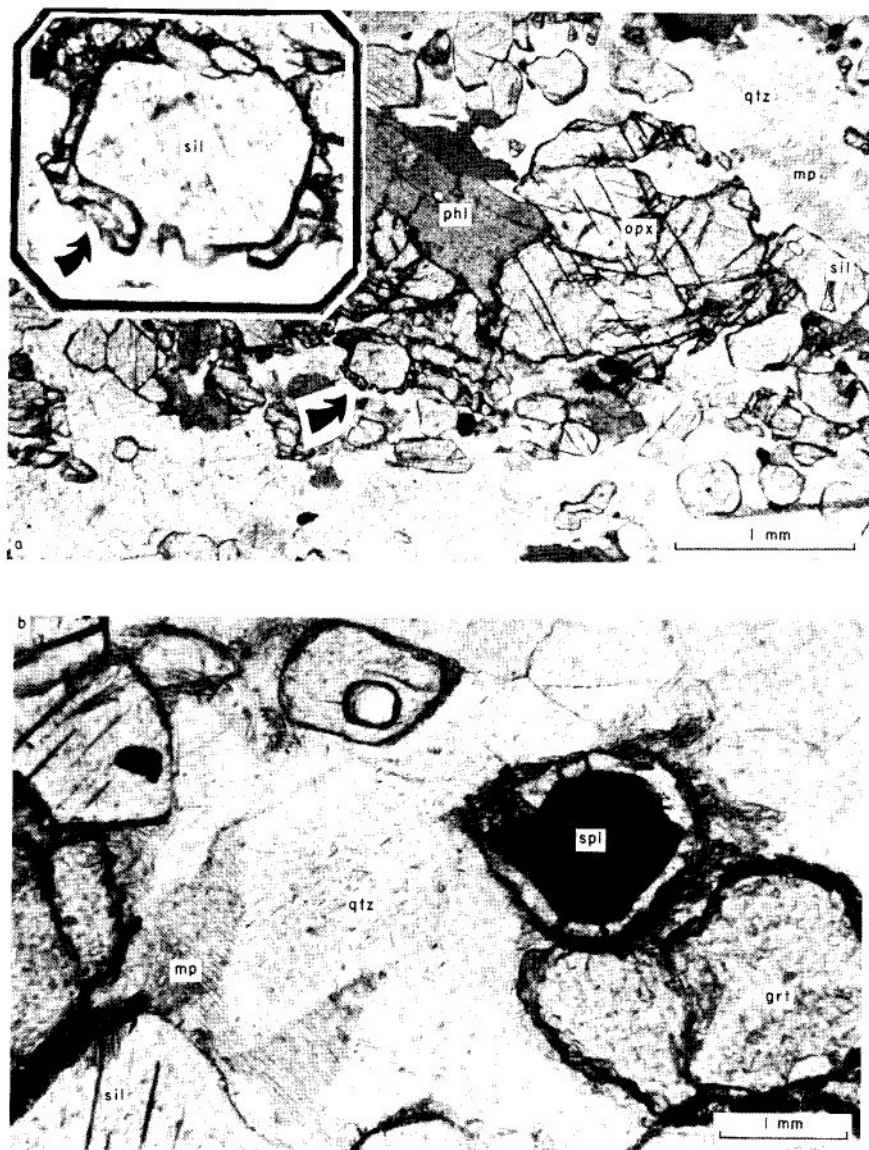


**Fig. 6a.**  $M_1$  sil–opx–mp–qtz assemblage in metapelite R25657. Inset shows secondary garnet corona on sillimanite, a texture developed during  $M_2$  phlogopite growth. **6b.**  $M_1$  sil–grt–qtz mp spl assemblage in metapelite R25641. Spinel and quartz are separated by a thin sillimanite corona.

the Napier Complex and suggest that the Fyfe Hills assemblages crystallized at higher pressures or lower temperatures than the cordierite-absent invariant point in KFMAS. However, as all mesoperthite in these assemblages contains appreciable albite as well as anorthite in mesoperthitic solid solution (Fig. 7), the absence of osumilite-bearing assemblages at Fyfe Hills may be a function of inappropriate bulk-compositions rather than of unusual P-T conditions (Grew, 1982a).

In summary, the metapelitic assemblages in the Fyfe Hills region imply  $M_1$  crystallization at temperatures close to, and pressures above, the spinel-absent invariant point in FMAS (Fig. 3b). Temperatures at Fyfe Hills must therefore have been close to the temperatures in the Tula Mountains (Ellis *et al.*, 1980; Grew, 1980, 1982b). In view of the possibility that Fyfe Hills assemblages crystallized near the cordierite-absent invariant point in KFMAS (Fig. 3a), Fyfe Hills

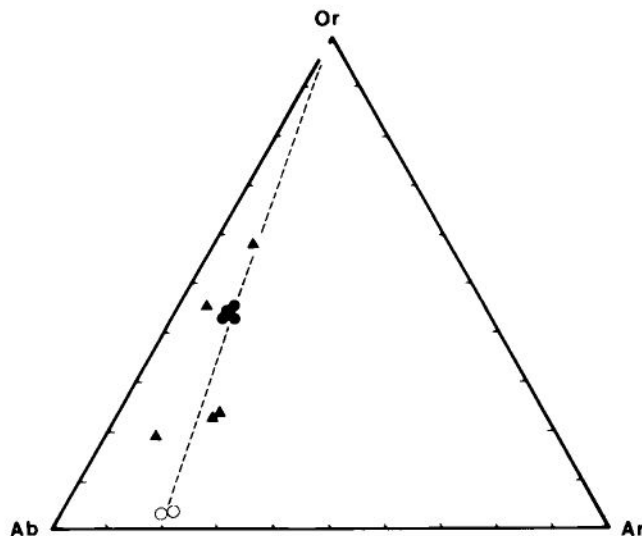


Fig. 7. Composition of mesoperthites in metapelites (triangles) and in charnockitic gneisses (solid circles). Open circles represent composition of exsolution lamellae.

**Table 8.** Geobarometry of granulite facies assemblages, Fyfe Hills

Event	Sample	$a_{An,pl}$	$a_{Gr,grt}$	$a_{Py,grt}$	$a_{En,opx}$	$\ln K^1$	$\ln K^2$	$P^1$	$P^2$
$M_1$	R25631 c	0.385	0.040			-6.759		8.2(8.4)	
	r	0.404	0.058			-5.810			
	R25660 c	0.205	0.023			-6.531		8.6(8.7)	
	R25824 c	0.475	0.058			-6.329		9.0(9.1)	
	r	0.406	0.491			-6.073			
	R25620 c	0.349	0.106	0.291	0.332		-2.554		8.8(9.0)
	r	0.442	0.115	0.276	0.337		-2.836		
	R25662 c	0.180	0.025	0.511	0.472		-2.585		8.7(9.0)
	r	0.154	0.025	0.504	0.487		-2.481		
	R25800 c	0.190	0.033	0.404	0.391		-2.623		8.5(9.0)
<i>Fyfe Hills M<sub>1</sub> average</i>	2018F* c	0.413	0.080	0.258	0.260		-3.002		6.9(7.2)
	<i>Tula Mountains average</i>					-6.539	-2.587	8.6(8.8)	8.7(9.0)
						-7.477	-3.002	7.0	6.9(7.2)
$M_1$ coronas	R25384B	0.353	0.214	0.122	0.107		-2.481		
	R31038	0.493	0.212	0.200	0.262		-2.715		
	R31130	0.527	0.209	0.222	0.260		-2.586		
	<i>Average corona</i>						-2.594		
$M_2$	R25624	0.080	0.012			-5.669		6.5(6.7)	
	R25387	0.484	0.211	0.164	0.226		-2.953		6.6(6.9)
	R25686	0.523	0.224	0.175	0.258		-2.973		6.5(6.6)
	R25856	0.448	0.218	0.169	0.219		-2.762		7.2(7.6)
	<i>Average M<sub>2</sub></i>						-2.896		6.8(7.0)

$K^1 = (a_{An,pl}/a_{Gr,grt})^3$ .  $K^2 = [(a_{Py,grt}^2 \cdot a_{Gr,grt})/(a_{An,pl} \cdot a_{En,opx})]$ .  $P^1$  = pressure (kbar) defined by Newton & Haselton's (1981) grt pl sil-qtz barometer;  $P^2$  = pressures (kbar) defined by Newton & Perkins' (1982) grt opx pl qtz barometer.  $M_1$  pressures estimated for 900°C;  $M_2$  pressures estimated for 640°C. Tula Mountains grt pl sil qtz assemblages after Grew (1980).

\* Mount Hardy (Tula Mountains) sample collected by Grew (Grew's sample number 2018F).

Pressures in parentheses calculated for mineral analyses in which  $Fe^{3+}$  has been calculated by stoichiometry. Full mineral analyses tabulated in Tables 2–5. c = core analysis; r = rim analysis.

pressures must have been somewhat higher than in the Tula Mountains. This conclusion is in accord with the results of a regional geobarometric study of the Napier Complex (Harley, 1983). Grew (1982b) suggested, on the basis of natural assemblages, that the spinel-absent invariant point in FMAS occurs at about 850°C and 6 kbar. This estimate is similar to experimental determinations in the MAS system (Newton, 1972; Newton, Charlu & Kleppa, 1974) and provides a minimum for the Fyfe Hills granulite facies metamorphism.

The anorthite content of mesoperthite in metapelites and in charnockitic gneisses attains values of up to 17 mol. % (Fig. 7). This suggests that  $M_1$  temperatures were somewhat greater than 900°C, and constrains  $P_{H_2O} \leq 0.5$  kbar (see discussion by Sheraton *et al.*, 1980).

Three Fyfe Hills  $M_1$  garnet-sillimanite-plagioclase-quartz assemblages (Table 8) yield an average  $\ln K^1 = -6.512$  (where  $K^1 = (a_{An,pl}/a_{Gr,gr})^3$ ; Newton & Haselton, 1981), which is equivalent to 8.6 kbar at 900°C. This estimate is 1.6 kbar higher than the pressures defined by identical assemblages from the Tula Mountains (Grew, 1980; Table 8). Three Fyfe Hills  $M_1$

garnet-orthopyroxene-plagioclase-quartz assemblages (Table 8) using the method of Newton & Perkins (1982) yield pressures nearly identical with the garnet-sillimanite plagioclase-quartz assemblages at 900°C. The pressures defined by the Fyfe Hills garnet orthopyroxene plagioclase-quartz assemblages are 1.8 kbar higher than pressures obtained from a similar assemblage from the Tula Mountains (Table 8).

### $M_1$ assemblages in Fe-rich metasediments

$M_1$  pyroxenes with compositions essentially confined to the pyroxene quadrilateral frequently contain exsolution lamellae (Fig. 8). In exsolution intergrowths (in which  $mg_{opx} > 0.48$ ) derived from metamorphic augite, orthopyroxene lamellae occur exclusively on (100) as thin (< 10 µm wide) lamellae and form less than 5 mode % of the bulk pyroxene. However, in Fe-rich metasediments composed of subequal proportions of quartz, magnetite, and pyroxene (with  $mg_{opx} < 0.43$ ), orthopyroxene lamellae comprise significantly more of the exsolved pyroxene aggregates, and occur as 2- to 4-mm wide '001' lamellae in addition to narrower (100) lamellae (Fig. 8).

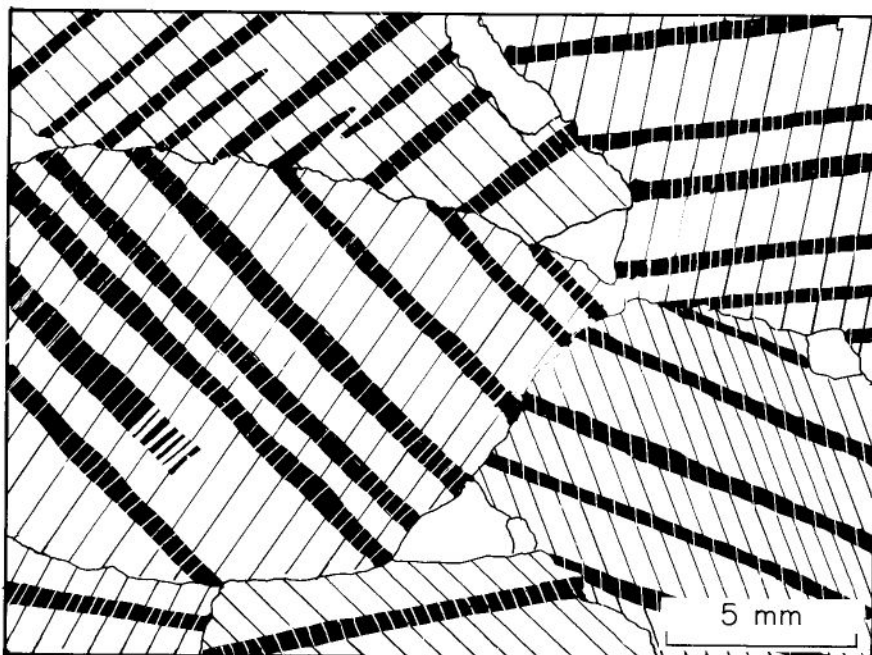


Fig. 8. Pyroxene exsolution structure in Fe-rich metasediment involving broad '001' clinopyroxene (light) and orthopyroxene lamellae (dark), as well as narrower (100) orthopyroxene and clinopyroxene lamellae. The '001' orthopyroxene lamellae represent inverted pigeonite lamellae. Pigeonite also occurs as very fine, submicroscopic, '001' lamellae in clinopyroxene.

The '001' orthopyroxene lamellae are inverted pigeonites (Robinson, 1980). The large size of these lamellae suggests, although does not prove, that exsolution occurred in the stability field of pigeonite rather than its metastable extension. The occurrence of pigeonite is noteworthy, as unusually high temperatures are required for its stabilization (Lindsley, 1983). Lindsley's (1983) thermometer yields a minimum temperature of about 1000°C at 9 kbar for the coexistence of pigeonite orthopyroxene-clinopyroxene at  $mg_{opx} = 0.43$  (Sandiford & Powell, unpublished data). As this assemblage occurs in undoubtedly metasediments, it cannot be attributed to a relic of igneous crystallization and, therefore, must be metamorphic in origin.

#### Preferred M<sub>1</sub> P-T range

The stability of sapphirine-quartz and sillimanite-hypersthene-quartz assemblages in systems approaching FMAS indicate that metamorphic temperatures exceeded 850°C at Fyfe Hills (see also Black *et al.*, 1983a). Even higher temperatures, close to 1000°C, are suggested by consideration of exsolution morphology in Fe-rich pyroxenes. Temperatures in excess of 850°C

are supported by a comparison of the assemblages observed at Fyfe Hills with other granulite terrains for which temperatures of 800–900°C have been estimated (cf. Wells, 1979; Warren, 1983; Phillips & Wall, 1981). In particular, the stability of sapphirine-mesoperthite-quartz at Fyfe Hills testifies to temperatures considerably higher than commonly attained in granulite terrains.

At temperatures of 915°C, coexisting garnet-sillimanite-plagioclase-quartz and garnet-orthopyroxene-plagioclase-quartz assemblages yield coincident pressures of 8.8 kbar ( $\pm 1.1$  and  $\pm 1.5$  kbar, respectively; Newton & Haselton, 1981; Newton & Perkins, 1982). These pressures are consistent with (1) the M<sub>1</sub> phase relations in metapelitic systems (Ellis *et al.*, 1980; Grew 1982a, 1982b); (2) the absence of garnet-clinopyroxene assemblages in meta-basic gneisses (Green & Ringwood, 1972); and (3) the occurrence of spinel-olivine clinopyroxene-orthopyroxene  $\pm$  Ti-hornblende in ultramafic gneisses (Green & Hibberson, 1970).

#### M<sub>2</sub> assemblages in meta-igneous gneisses

In mafic and felsic gneisses both garnet and hornblende form part of the M<sub>2</sub> assemblage

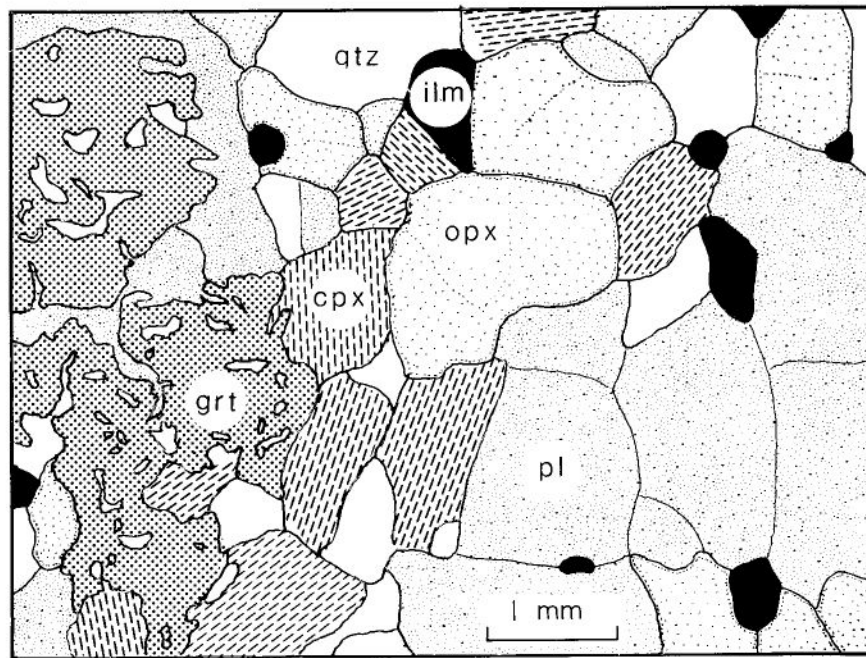


**Fig. 9.** M<sub>2</sub> grt-pl-opx-cpx-qtz ilm assemblage in metamorphosed tholeiitic dyke R25387. As is typical of M<sub>2</sub> garnet-bearing assemblages, garnet does not show the textural equilibration of the other components of the assemblage.

and occur with orthopyroxene (and/or clinopyroxene)-plagioclase (and/or K-feldspar)-quartz-ilmenite. In these samples garnet is rarely in textural equilibrium with both clinopyroxene and orthopyroxene (Fig. 9), and thus the M<sub>2</sub> assemblage garnet-clinopyroxene-orthopyroxene-plagioclase-quartz may not represent

equilibrium (as has, for instance, been suggested for similar occurrences in other granulites; de Waard, 1965). However, the garnet and pyroxene compositions do not vary significantly on the thin-section scale and hence the assumption of chemical equilibrium may be justified (see below). Relics of M<sub>1</sub> assemblages are frequently preserved

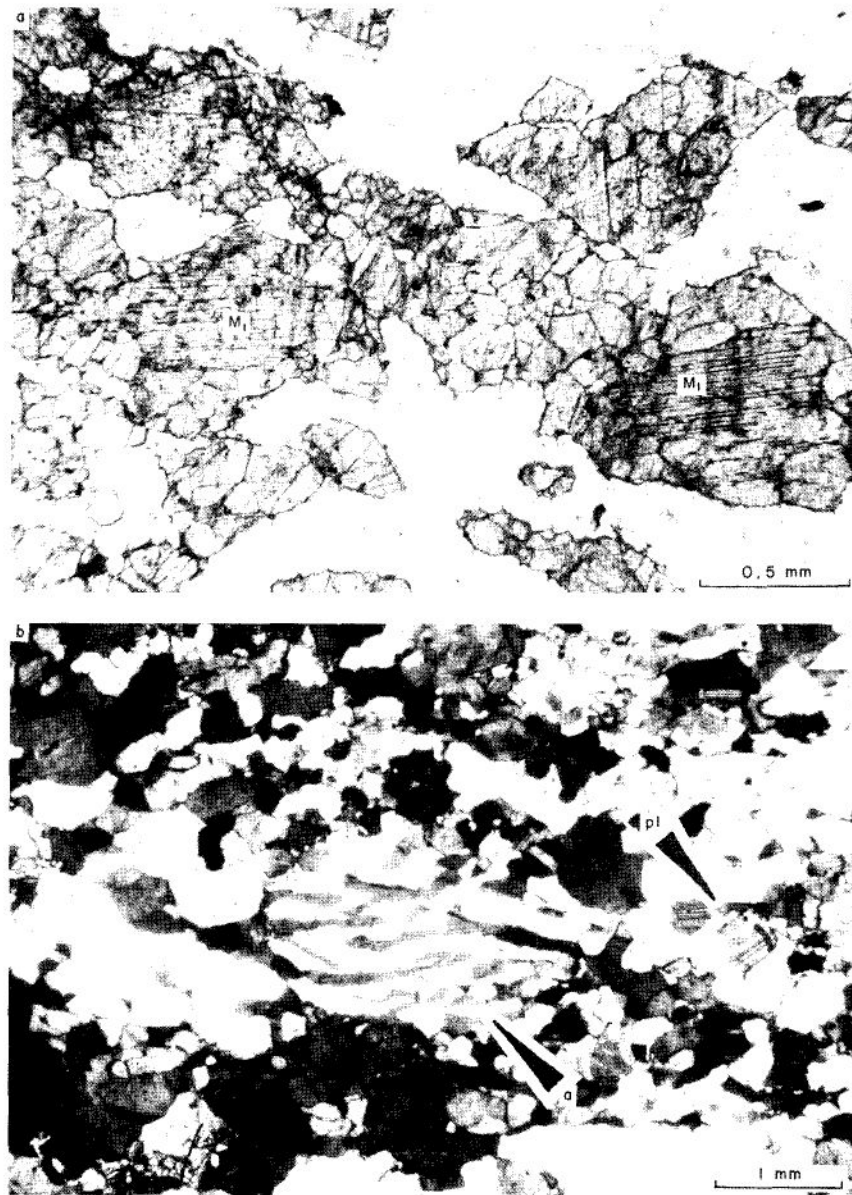


**Fig. 10a.** M<sub>1</sub> clinopyroxene (M<sub>1</sub>) surrounded by mantles of M<sub>2</sub> clinopyroxene in zone of partial M<sub>2</sub> recrystallization. Note that M<sub>1</sub> clinopyroxene contains prominent orthopyroxene exsolution lamellae on (100) (darker lines), whereas exsolution lamellae are not well developed in M<sub>2</sub> clinopyroxene. **10b.** Deformed antiperthite (a) in zone of partial M<sub>2</sub> recrystallization. During M<sub>2</sub> recrystallization, plagioclase and orthoclase formed at the expense of the M<sub>1</sub> ternary feldspar.

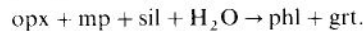
in zones transitional to  $M_2$  (Fig. 10a,b). In these samples, the  $M_2$  feldspars and pyroxenes contrast their  $M_1$  counterparts in that they contain few exsolution lamellae. Thus,  $M_2$  assemblages must have crystallized at temperatures substantially lower than  $M_1$ .

Wells' (1977)  $M_2$  temperature estimates (Table 7) are 80–100°C lower than the  $M_1$  estimates. They are 50–80°C higher than Ganguly's (1979) garnet clinopyroxene temperatures and 140–170°C higher than Ellis & Green's (1979) garnet–clinopyroxene temperatures in the same assemblage (Table 7). In view of the evidence that the Ellis & Green (1979) garnet–clinopyroxene temperatures define the most reasonable temperatures for crustal metamorphics (Essene, 1982) at temperatures below about 850–900°C (below which the pyroxene-solvus thermometers are notoriously insensitive to temperature; Essene, 1982), the preferred  $M_2$  temperature range is  $640 \pm 50^\circ\text{C}$ , an estimate which is similar to the preferred temperatures of Harley (1983) and Black *et al.* (1983b).

Traditionally, the appearance of garnet in mafic granulites has been attributed to high pressures (de Waard, 1965; Green & Ringwood, 1972). However, Percival (1983) has suggested that garnet–clinopyroxene assemblages are stable in the transition between amphibolites and orthopyroxene-bearing granulites in a normal prograde sequence. Thus, the presence of garnet in mafic and intermediate meta-igneous gneisses may not, in itself, be considered indicative of unusually high pressures in granulite terrains. This conjecture is consistent with the average  $\ln K^2$  ( $K^2 = a_{\text{Gr.grt}} \cdot (a_{\text{Py.grt}})^2 / a_{\text{An.pl}} \cdot a_{\text{En.opx}}$ ) for  $M_2$  garnet plagioclase–orthopyroxene–quartz assemblages of  $-2.896$  (Table 8), which, at  $640^\circ\text{C}$ , is equivalent to a pressure of  $6.8 \pm 1.5$  kbar (Newton & Perkins, 1982).

### $M_2$ assemblages in metapelites

Phlogopite-rich zones which transgress metapelites at Fyfe Hills are attributed to rehydration and recrystallization during  $M_2$  (Sandiford & Wilson, 1984; Black *et al.*, 1983b). The partitioning of Fe between the ferro-magnesian phases in these metapelites ( $\text{mg}_{\text{phl}} > \text{mg}_{\text{opx}} > \text{mg}_{\text{grt}}$ ), and the textual relations (Fig. 3e) suggest the principal phlogopite producing reaction was



In assemblages where the  $M_1$  mesoperthite contained significant anorthite component, the phlogopite producing reaction involved the production of plagioclase. The compositions of

garnet and plagioclase in one such  $M_2$  garnet–plagioclase–sillimanite–quartz assemblage (R25624) yield a  $\ln K^1 = -5.669$  (Table 8), which is equivalent to  $6.5 \pm 1.1$  kbar at  $640^\circ\text{C}$  (Newton & Haselton, 1981). The equivalence of garnet–sillimanite–plagioclase–quartz and garnet plagioclase–orthopyroxene–quartz pressures at  $640^\circ\text{C}$  provides support for the validity of the Ellis & Green (1979) temperature estimates and justification for the assumption of chemical equilibrium between garnet and pyroxenes in  $M_2$  metaigneous assemblages.

### METAMORPHIC CONDITIONS DURING RSZ FORMATION

The metamorphic and structural evolution of RSZs at Fyfe Hills is described in detail by Sandiford (1985) and is only briefly summarized here. The earliest formed assemblages recognized in the RSZs ( $M_3$ ) include gedrite–kyanite–quartz, and are estimated to have formed at 5.5–8 kbar and  $620$ – $720^\circ\text{C}$ . Subsequent deformation within the retrograde zones occurred at shallower levels (at depth equivalents of 3–5 kbar) at more or less constant temperature. Near-isothermal decompression during the evolution of the RSZs is witnessed by reaction textures in which early formed kyanite and gedrite are mantled by cordierite. This is interpreted as evidence that significant thickening of the Enderby Land crust occurred during RSZ formation (Sandiford, 1985).

### P-T-t TRAJECTORIES FOR THE FYFE HILLS GNEISSES

The preferred P-T estimates for the two granulite facies events and the amphibolite facies RSZ events provide a number of fields in P-T space through which the Fyfe Hills sequence passed during their metamorphic evolution. These fields are consistent with a P-T-t trajectory involving either: prolonged deep-crustal residence from  $M_1$  in the mid to late Archaean through to the initiation of the RSZ in the late Proterozoic, or successive episodes of excavation from, and burial to, depth equivalents of 5.5 kbar or more. To determine which alternative applies, mineral reaction features formed in the static intervals between these metamorphic events are considered below.

#### Post- $M_1$ mineral reaction textures

Reaction textures are commonly developed between the component minerals of  $M_1$  assemblages (Figs 11, 12). Many of these textures involve solid–solid equilibria and thus imply partial re-equilibration to changing P-T conditions.

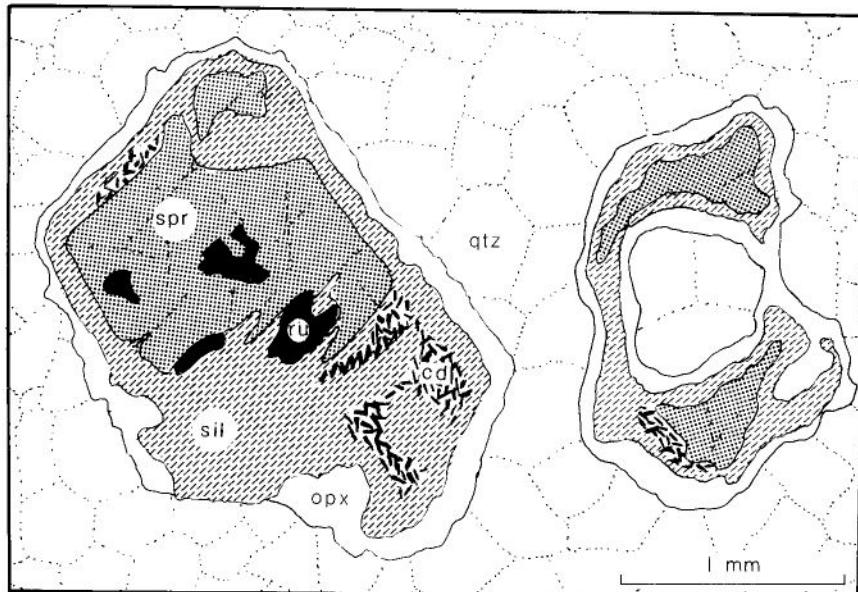


**Fig. 11.** Sil-opx corona around sapphirine in  $M_1$  spr-quartz-ru assemblage (R31180). Corundum (cd) also occurs in the corona assemblage but is never in contact with orthopyroxene.

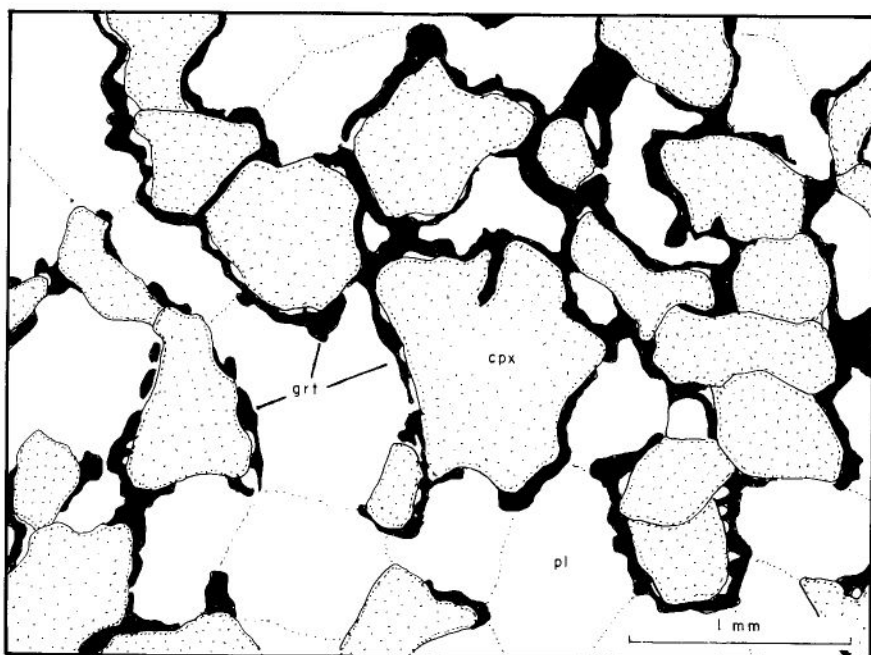
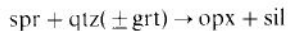


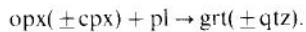
**Fig. 12.** Garnet corona on clinopyroxene in the  $M_1$  cpx-pl assemblage (R31136).

A regime of near-isobaric cooling at temperatures as high as 800–850°C is indicated by the occurrence of sillimanite–orthopyroxene coronas between sapphirine–quartz ± garnet assemblages in rocks with compositions approximating FMAS (Fig. 11). The absence of cordierite in reaction coronas in systems approximating FMAS, and the positive P–T slope (Fig. 11) of equilibria defined by the reaction (Morse & Talley, 1971)



indicates that this reaction occurred at temperatures above the spinel-absent invariant point in FMAS (i.e. above 850°C and 6 kbar; Grew, 1982a), in response to cooling at constant, increasing or only slightly decreasing pressures. The high alumina-content orthopyroxene coronas in R31180 (total Al/total cations = 0.083;  $\text{Fe}^{2+}/(\text{Fe}^{2+} + \text{Mg}) = 0.25$ ) suggests temperatures of corona crystallization in the range 850–900°C (Anastasiou & Seifert, 1972; Grew, 1980). Such high temperatures for this near-isobaric reaction segment suggest the coronas formed soon after  $M_1$  at a temperature well above, and consequently prior to,  $M_2$ .

Some support for post- $M_1$  isobaric cooling may be provided by coronas of garnet ± quartz on  $M_1$  orthopyroxene and/or clinopyroxene in plagioclase-bearing assemblages (Fig. 12), although it is not clear that these textures developed prior to  $M_2$  (Sandiford & Wilson, 1984). The texture indicates the post- $M_1$  reaction,



Rim compositions of orthopyroxene and plagioclase adjacent to the corona yield variable  $\ln K^2$  values (Table 8). The average  $\ln K^2 = -2.896$ , and is almost identical to the average  $M_1 \ln K^2$  (Table 8). Because lines of constant  $\ln K^2$  (isopleths) have low positive  $dT/dP$  slopes (64°C/kbar; Fig. 13), these reaction coronas probably developed at pressures slightly lower and temperatures substantially lower than  $M_1$ .

In one sample (R25817), garnet forming part of the  $M_1$  assemblage garnet–orthopyroxene–plagioclase is surrounded by a symplectitic intergrowth of secondary plagioclase–orthopyroxene (Fig. 14). The symplectitic intergrowth of orthopyroxene and plagioclase has subsequently reacted to garnet (Fig. 14). The earlier reaction texture may have formed in response to (1) prograde heating of  $M_1$  assemblages which continued after the cessation of deformation; or (2) pressure reduction at constant, increasing, or only slightly decreasing temperature after  $M_1$ . In either case,

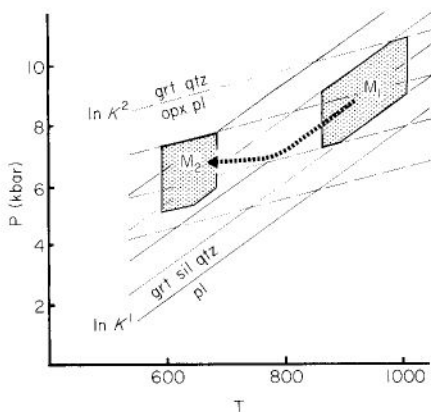


**Fig. 13.** Isopleths for Fyfe Hills garnet–plagioclase–sillimanite–quartz (continuous lines) and garnet–plagioclase–orthopyroxene–plagioclase–quartz equilibria (dashed lines). Preferred  $M_1$  and  $M_2$  P–T fields marked in heavy lines. Heavy dashed line represents a P–T–t path consistent with observed zoning profiles and corona development (see text).

the occurrence of the secondary garnet corona is consistent with the interpretation that the metamorphic evolution of this specimen included a period of cooling at moderate to deep crustal levels.

#### Mineral zoning

Mineral zoning in  $M_1$  garnet–sillimanite–plagioclase–quartz and garnet–orthopyroxene–plagioclase–quartz assemblages has been investigated to determine the response of these pressure-sensitive systems to retrograde metamorphic evolution (Table 8). Although it is doubtful that rim compositions in these assemblages attained equilibrium at any one set of P–T conditions, the general nature of zoning profiles should reflect general changes in the thermal and baric regime following the equilibration of the  $M_1$  assemblage.

Rimward zoning in  $M_1$  garnet–sillimanite–plagioclase–quartz assemblages is towards lower  $\ln K^1$  values (average rim  $\ln K^1 = -5.959$  compared with average core  $\ln K^1 = -6.539$ ; Table 8); that is towards lower T or higher P configurations. At  $\ln K^1 = -5.959$ , pressures in excess of 6 kbar are implied by temperatures of 640°C or more (Newton & Haselton, 1981). Rimward zoning in  $M_1$  garnet–orthopyroxene–plagioclase–quartz assemblages is inconsistent (Table 8): R25629 zones towards a lower P and/or higher T configuration, while R25662 zones towards a higher P and/or lower T configuration.

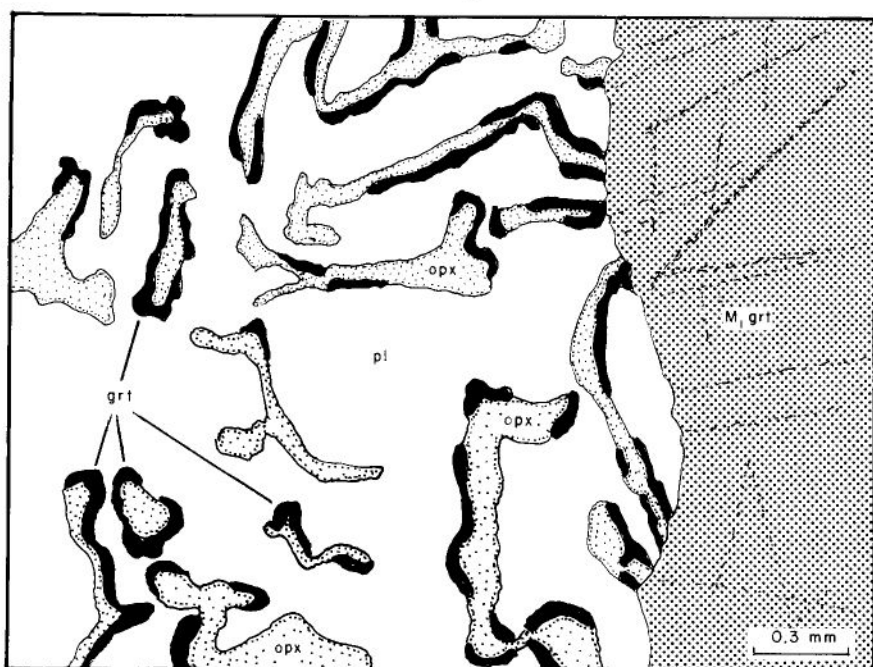


**Fig. 14.** Post- $M_1$  orthopyroxene-plagioclase symplectite surrounding  $M_1$  garnet in garnet-orthopyroxene-plagioclase assemblages (R25817). Secondary garnet occurs in coronas on the orthopyroxene-plagioclase symplectite.

The anomalous zoning profiles in these samples may be due to the failure of the garnet-orthopyroxene-plagioclase quartz rims to attain equilibrium or may reflect closure of different rim-reaction systems at different stages of the post- $M_1$  P-T-t trajectory. Because of the shallow positive slope of both Mg and Fe end-member isopleths in the system garnet-orthopyroxene-plagioclase-quartz in P-T space (Newton & Perkins, 1982; Bohlen, Wall & Boettcher, 1983) slight variations in  $dP/dT$  during cooling at slightly decreasing pressures may produce either an increase or decrease in  $\ln K^2$  (Fig. 13). Due to the somewhat greater temperature dependence of garnet-sillimanite-plagioclase-quartz equilibria (Newton & Haselton, 1981), this P-T-t trajectory would produce only decreasing  $\ln K^1$  values (Fig. 13). Additional support for the P-T path illustrated in Fig. 13 is provided by the atypical orthopyroxene-plagioclase symplectite (Fig. 14), which may have formed during the initial cooling segment with the relatively steep  $dP/dT$  and the secondary garnet corona forming during the subsequent shallower  $dP/dT$  cooling segment.

Thus, in general, the rimward zoning in  $M_1$  pressure-sensitive equilibria confirms the interpretation, based on reaction textures, that  $M_1$  was

followed by cooling at constant or only slightly decreasing pressure.

#### Preferred P-T-t trajectory for the Fyfe Hills granulites

Mineral reaction textures and mineral zoning profiles superimposed on  $M_1$  assemblages imply that the P-T-t path between the crystallization of  $M_1$  and  $M_2$  assemblages did not involve the excavation of the gneissic sequence to crustal levels less than the depth equivalent of 5.5–6 kbar. The orthopyroxene-plagioclase symplectite on  $M_1$  garnet (Fig. 14) and the anomalous zoning profiles in garnet-orthopyroxene-plagioclase-quartz assemblages suggest that this  $M_1$ - $M_2$  P-T-t path may have bowed towards the temperature axis (Fig. 13). However, the crossing of reactions with positive  $dP/dT$  during cooling implies that at pressures in excess of 5.5–6 kbar the Fyfe Hills gneisses remained at a constant crustal level (thereafter cooling continued isobarically). Furthermore, the similarities in the pressures recorded by  $M_2$  assemblages, by RSZ assemblages (Sandiford, 1985), suggests that the Fyfe Hills granulites remained at the depth equivalent of about 5.5–8 kbar from the late Archaean through to the late Proterozoic.

The preferred P-T path for the Fyfe Hills granulites corresponds in form to the general post-peak P-T evolution of the Napier Complex proposed by Sheraton *et al.* (1980) and Ellis (1980) and to the detailed P-T paths for specific localities in the Napier Complex described by Ellis (1983) and Harley (1983).

## DISCUSSION

The geothermometric and petrographic data indicate that the sapphirine-mesoperthite-quartz and related granulites at Fyfe Hills crystallized at temperatures rarely encountered in exposed granulite terrains. Indeed, as the 850–1000°C temperatures inferred for the Fyfe Hills assemblages closely approach the temperature required for 'dry' melting of felsic granulite (Huang & Wyllie, 1975), they must represent the upper limit for crustal metamorphism.

The preferred P-T-t trajectory for the Fyfe Hills gneisses (Fig. 13) implies that cooling from the unusually high temperatures occurred at constant or only slightly decreasing pressures in excess of 5.5–6 kbar. This P-T-t trajectory is supported by (1) evidence for repeated retrograde metamorphism at depth equivalents of 5.5–8 kbar; (2) mineral reaction coronas on M<sub>1</sub> granulite assemblages indicative of cooling at pressures in excess of 6 kbar; and (3) mineral zoning profiles towards compositions which are (generally) indicative of conditions of lower apparent T/P.

The evidence for extended deep crustal residence during a regime of near-isobaric cooling implies that the M<sub>1</sub> granulite facies event occurred during a regime of perturbed heat flow (with the 'metamorphic geotherm' of about 30°C/km). Metamorphism during unusually high heat flow at moderate to deep crustal levels most probably results from thermal input associated with mantle derived magmas (Ellis, 1980; Wells, 1980). As granulite metamorphism at Fyfe Hills occurred at least 0.7 Ga (Black *et al.*, 1983a) and possibly as much as 1.3 Ga (DePaolo *et al.*, 1982) after the deposition of the supracrustal sequence, radioactive decay within the metamorphic pile cannot have provided the sole heat source for this metamorphic event (DePaolo *et al.*, 1982). Despite differential erosion of some 6–8 km, the similar temperatures recorded by assemblages in both the Tula Mountains and the Fyfe Hills region strongly support regional magmatic accretion during metamorphism. Indeed, Wells' (1980) model of pulsed 'overaccretion' at magmatic temperatures of 1000°C lasting 10 Ma predicts maximum temperatures in the range of 850–900°C

for all crustal levels below about 25 km, in accord with the regional P-T conditions deduced for the Napier Complex. This interpretation is in accord with compelling field evidence for extensive magmatic activity during granulite facies metamorphism in the Napier Complex (Sandiford & Wilson, 1983; Sheraton & Black, 1983).

The 'geotherm' recorded by Fyfe Hills M<sub>1</sub> assemblages (approximately 30°C/km) is, like many other Archaean granulites (Wells, 1979), similar to modern day near-surface geotherms in many Precambrian shields. However, the relative distribution and contribution of radioactive elements in the upper most crust (which imparts a marked temperature convexity to the ambient crustal geotherm) implies that the near-surface geotherm during the granulite facies metamorphism at Fyfe Hills was substantially higher, and probably in the vicinity of 40–50°C/km (Drury, 1978). It is likely, therefore, that the thermal regime of the Enderby Land crust was significantly 'hotter' than modern day cratons. Indeed, a markedly convex 'granulite geotherm' for the Napier Complex is suggested by the Tula Mountains assemblages which record a 'geotherm' of about 37°C/km. Regional variations in the P-T may alternatively reflect diachronous crystallization of peak assemblages, in which case the different exposures reflect the polychronic evolution of the Napier 'metamorphic geotherm' (England & Richardson, 1977; Wells, 1980).

Successive retrograde metamorphic events documented at Fyfe Hills occurred at approximately constant depth and constant temperature. The mid-crustal 'geotherm' recorded by these events (20–34°C/km) is considerably higher than the predicted geotherm at similar crustal levels in modern day tectonically stable crusts (approximately 17°C/km; Clarke & Ringwood, 1964), and suggests that these metamorphic events represent thermal perturbations in the middle crust. However, in light of the possibility that the thermal character of the middle and lower crust has changed considerably since the Precambrian (Schubert, Stevens & Cassen, 1980), such P-T conditions are not unreasonable for steady-state conditions. An increase in the temperature of the base of the continental crust of 50–100°C per 1000 Ma (Schubert *et al.*, 1980), would imply steady-state lower crustal geotherms of 18–22°C and 22–26°C for the late Proterozoic and late Archaean, respectively. These thermal regimes are in the ranges defined by P-T estimates for retrograde metamorphic events at Fyfe Hills, and are consistent with the interpretation that these events occurred during a steady state thermal

regime lasting from the late Archaean to the late Proterozoic.

As prolonged isobaric cooling implies that a steady-state crustal thickness has been attained, it is possible to constrain the crustal thickness variations with time at Fyfe Hills. Modern continental shields away from continental edge effects typically have 35–40 km thick crusts (Condie, 1976). By analogy, the crust at Fyfe Hills is considered to have been 35–40 km thick during the interval of isobaric cooling (assuming that any decrease in the steady state continental geotherm since the late Archaean has not substantially affected the nature of continental isostatic compensation). As the Fyfe Hills gneisses were at this time at a depth of 18–26 km, the depth to the Moho beneath the Fyfe Hills structural level would have been in the range of 9–22 km. The Fyfe Hills gneisses therefore represent deep crust metamorphosed close to the base of a continent. Furthermore, as the burial depths indicated by  $M_1$  assemblages are in the range 26–34 km, the thickness of the Fyfe Hills crust during granulite facies metamorphism must have been in the range of 35–56 km.

Groushinsky & Sazhina (1982) estimated the crustal thickness in the Fyfe Hills–Amundsen Bay region to be approximately 35 km. The estimates for the total crustal thickness during the granulite facies metamorphism are 13–26 km less than the cumulative crustal thickness (60–70 km) obtained by summing the current depth of exposure plus the present crustal thickness. This disparity suggests that the crust at Fyfe Hills has undergone considerable post-granulite facies thickening. Extensive crustal thickening during the late Proterozoic during RSZ formation in the Fyfe Hills region is suggested by assemblages in these shear zones, indicative of near-isothermal excavation of the gneisses from deep crustal levels (Sandiford & Wilson, 1983; Sandiford, 1985).

In summary, the recognition that granulite facies metamorphism at Fyfe Hills was followed by prolonged deep crustal residence during a period of near-isobaric cooling implies that granulite metamorphism occurred near the base of a crust of moderate thickness. In light of the Fyfe Hills evidence, some concern must be expressed about previous estimates of Archaean crustal thickness based on simple addition of the current depth of exposure plus the underlying crust (Windley, 1977; Wells, 1981; England & Bickle, 1984). Moreover, the correlation of Archaean granulite terrains with modern day convergent margin settings (Windley, 1977) based on inferred similarities in crustal thickness must be questioned in light of the Fyfe Hills data.

## ACKNOWLEDGEMENTS

The rocks described in this paper were collected during the 1979–80 ANARE expedition. Logistic support provided by the Antarctic Division of the Department of Science is gratefully acknowledged. 'In field' discussions with C. J. L. Wilson, E. S. Grew, and S. L. Harley are gratefully appreciated. R. Powell is thanked for reviewing an earlier draft of the manuscript.

## REFERENCES

- Anastasiou, P. & Seifert, F., 1972. Solid solubility of  $\text{Al}_2\text{O}_3$  in enstatite at high temperatures and 1–5 kbar water pressure. *Contr. Miner. Petrol.*, **34**, 272–287.
- Black, L.P. & James, P.R., 1983. Geological history of the Archaean Napier Complex. In *Antarctic Earth Science* (ed. Oliver, R.L., James, P.J. & Jago, J.B.), pp. 11–15. Australian Academy of Science, Canberra.
- Black, L.P., James, P.R. & Harley, S.L., 1983a. Geochronology and structure of the early Archaean rocks at Fyfe Hills, Enderby Land, Antarctica. *Precambr. Res.*, **21**, 197–222.
- Black, L.P., James, P.R. & Harley, S.L., 1983b. Geochronology and geological evolution of metamorphic rock in the Field Islands area, East Antarctica. *J. metamorphic Geol.*, **1**, 277–303.
- Bohlen, S.R., Wall, V.J. & Boettcher, A.L., 1983. Experimental investigation and application of model garnet granulite equilibria. *Contr. Miner. Petrol.*, **83**, 52–61.
- Clarke, S. P. & Ringwood, A. E., 1964. Density distribution and constitution of the mantle. *Riv. Geophys.*, **2**, 35–88.
- Compton, W. & Williams, I.S., 1982. Protolith ages from inherited zircon cores measured by a high mass resolution ion microprobe. *Fifth int. Conf. Geochronology, Cosmochronology and Isotope Geology, Nikko, Japan, 1982*. Abstract 63–64.
- Condie, K.C., 1976. *Plate Tectonics and Crustal Evolution*. Pergamon, Oxford.
- de Waard, D., 1965. The occurrence of garnet in granulite-facies terrain of the Adirondack Highlands. *J. Petrology*, **6**, 165–191.
- Depaolo, D.J., Manton, W.I., Grew, E.S. & Halpern, M., 1982. Sm-Nd, Rb-Sr and U-Th-Pb systematics of granulite facies gneisses from Fyfe Hills, Enderby Land, Antarctica. *Nature, Lond.*, **298**, 614–618.
- Drury, S.A., 1978. Were Archaean continental geothermal gradients much steeper than today? *Nature, Lond.*, **274**, 720.
- Ellis, D.J., 1980. Osumilite–sapphirine quartz granulites from Enderby Land, Antarctica: P-T conditions of metamorphism, implications for garnet–cordierite equilibria and the evolution of the deep crust. *Contr. Miner. Petrol.*, **74**, 201–210.
- Ellis, D.J., 1983. The Napier and Rayner Complexes of Enderby Land, Antarctica – contrasting styles of metamorphism and tectonism. In *Antarctic Earth Science* (ed. Oliver, R.L., James, P.J. & Jago, J.B.), pp. 20–24. Australian Academy of Science, Canberra.
- Ellis, D.J. & Green, D.H., 1979. An experimental study of the effect of Ca upon garnet–clinopyroxene

- Fe-Mg exchange equilibria. *Contr. Miner. Petrol.*, **71**, 13–22.
- Ellis, D.J., Sheraton, J.W., England, R.N. & Dallwitz, W.B., 1980. Osumilite sapphirine-quartz granulites from Enderby Land, Antarctica—mineral assemblages and reactions. *Contr. Miner. Petrol.*, **72**, 123–143.
- England, P.C. & Bickle, P., 1984. Continental thermal and tectonic regimes during the Archaean. *J. Geol.*, **92**, 353–367.
- England, P.C. & Richardson, S.W., 1977. The influence of erosion upon the mineral facies of rocks from different metamorphic environments. *J. geol. Soc. Lond.*, **134**, 201–213.
- Essene, E.I., 1982. Geological thermometry and barometry. *Rev. Miner.*, **10**, 153–206.
- Ferguson, A.K. & Sewell, D.K.B., 1980. A peak integration method for acquiring X-ray data for on-line microprobe analysis. *X-ray spectra*, **9**.
- Ganguly, J., 1979. Garnet and clinopyroxene solid solutions and geothermometry based on Fe-Mg distribution coefficients. *Geochim. cosmochim. Acta*, **43**, 1021–1029.
- Green, D.H. & Hibberson, W., 1970. The instability of plagioclase in peridotite at high pressure. *Lithos*, **3**, 209–221.
- Green, D.H. & Ringwood, A.E., 1972. A comparison of the recent experimental data on the gabbro-garnet granulite eclogite transition. *J. Geol.*, **80**, 277–288.
- Grew, E.S., 1978. Precambrian basement at Molodezhnaya Station, East Antarctica. *Bull. geol. Soc. Am.*, **89**, 801–813.
- Grew, E.S., 1980. Sapphirine-quartz association from the Archaean rocks of Enderby Land, Antarctica. *Am. Miner.*, **65**, 821–836.
- Grew, E.S., 1982a. Osumilite in the sapphirine-quartz terrain of Enderby Land, East Antarctica: implications for osumilite petrogenesis in the granulite facies. *Am. Miner.*, **67**, 762–787.
- Grew, E.S., 1982b. Sapphirine, kornerupine, and sillimanite and orthopyroxene in the charnockitic region of south India. *J. geol. Soc. India*, **23**, 469–505.
- Groushinsky, N.P. & Sazhina, N.B., 1982. Some features of Antarctic crustal structure. In *Antarctic Geoscience* (ed. Craddock, C.), pp. 907–911. Wisconsin Press, Madison.
- Harley, S.L., 1981. Garnet orthopyroxene assemblages as pressure indicators. *Ph.D. thesis, University of Tasmania*.
- Harley, S.L., 1983. Regional geobarometry-geothermometry and metamorphic evolution of Enderby Land, Antarctica. In *Antarctic Earth Science* (ed. Oliver, R.L., James, P.R. & Jago, J.B.), pp. 25–30. Australian Academy of Science, Canberra.
- Huang, W.L. & Wyllie, P.J., 1975. Melting relations in the system  $\text{NaAlSi}_2\text{O}_8-\text{KAlSi}_3\text{O}_8-\text{SiO}_2$  to 35 kilobars, dry and with excess water. *J. Geol.*, **83**, 737–748.
- Lindsley, D.H., 1983. Pyroxene thermometry. *Am. Miner.*, **68**, 477–493.
- Morse, S.A. & Talley, J.H., 1971. Sapphirine reactions in deep-seated granulites near Wilson Lake, Central Labrador, Canada. *Earth planet. Sci. Lett.*, **10**, 325–328.
- Newton, R.C., 1972. An experimental determination of the high pressure stability limits of cordierite under wet and dry conditions. *J. Geol.*, **80**, 398–420.
- Newton, R.C., Charlu, T.V. & Kleppa, O.J., 1974. A calorimetric investigation of the high-pressure stability of anhydrous magnesium cordierite with application to granulite facies metamorphism. *Contr. Miner. Petrol.*, **44**, 295–311.
- Newton, R.C. & Haselton, H.T., 1981. Thermodynamics of garnet-plagioclase- $\text{Al}_2\text{O}_3$ -quartz geobarometer. In *Thermodynamics of Minerals and Melts* (ed. Newton, R.C., Navrotsky, A. & Wood, B.J.), pp. 231–247. Springer-Verlag, New York.
- Newton, R.C. & Perkins, D., 1982. Thermodynamic calibration of geobarometers based on the assemblage garnet plagioclase-orthopyroxene (clinopyroxene)-quartz. *Am. Miner.*, **67**, 203–222.
- O'Hara, M.J., 1977. Thermal history of excavation of Archaean gneisses from the base of the crust. *J. geol. Soc. Lond.*, **134**, 185–200.
- Percival, J.A., 1983. High-grade metamorphism in the Chapleau Foleyet Area, Ontario. *Am. Miner.*, **68**, 667–686.
- Phillips, G.N. & Wall, V.J., 1981. Evaluation of prograde regional metamorphic conditions: their implications for heat source and water activity during metamorphism in the Willyama Complex, Broken Hill, Australia. *Bull. Miner.*, **104**, 801–810.
- Robinson, P., 1980. The composition space of terrestrial pyroxenes: internal and external limits. *Rev. Miner.*, **7**, 419–494.
- Sandiford, M., 1985. The origin of retrograde shear zones in the Napier Complex: implications for the tectonic evolution of Enderby Land. *J. structural Geol.*, **7**, 477–488.
- Sandiford, M. & Wilson, C.J.L., 1983. The geology of the Fyfe Hills Khmara Bay region. In *Antarctic Earth Science* (ed. Oliver, R.L., James, P.R. & Jago, J.B.), pp. 16–19. Australian Academy of Science, Canberra.
- Sandiford, M. & Wilson, C.J.L., 1984. The structural evolution of the Fyfe Hills–Khmara Bay region, Enderby Land, East Antarctica. *Aust. J. Earth Sci.*, **31**, 403–426.
- Schubert, G., Stevans, D. & Cassen, P., 1980. Whole planet cooling and radiogenic heat source contents of the earth and moon. *J. geophys. Res.*, **85**, 2531–2583.
- Sheraton, J.W. & Black, L.P., 1981. Geochemistry and geochronology of Proterozoic tholeiitic dykes of east Antarctica: evidence for mantle metasomatism. *Contr. Miner. Petrol.*, **78**, 305–317.
- Sheraton, J.W. & Black, L.P., 1983. Geochemistry of Precambrian gneisses: relevance for the evolution of the East Antarctic Shield. *Lithos*, **16**, 273–296.
- Sheraton, J.W., Offe, L.A., Tingey, R.J. & Ellis, D.J., 1980. Enderby Land, Antarctica—an unusual Precambrian high grade terrain. *J. geol. Soc. Aust.*, **27**, 1–18.
- Warren, R.G., 1983. Metamorphic and tectonic evolution of granulite, Arunta Block, central Australia. *Nature. Lond.*, **305**, 300–303.
- Wells, P.R.A., 1977. Pyroxene thermometry in simple and complex systems. *Contr. Miner. Petrol.*, **62**, 129–139.
- Wells, P.R.A., 1979. Chemical and thermal evolution of

- Archaean sialic crust, South West Greenland. *J. Petrology*, **20**, 187–226.
- Wells, P.R.A., 1980. Thermal models for the magmatic accretion and subsequent metamorphism of continental crust. *Earth planet. Sci. Lett.*, **46**, 253–265.
- Wells, P.R.A., 1981. Accretion of the continental crust: thermal and geochemical consequences. *Phil. Trans. R. Soc. Lond. A*, **301**, 347–357.
- Windley, B.F., 1977. Timing of continental emergence. *Nature, Lond.*, **270**, 426–428.
- Wood, B.J. & Banno, S., 1973. Garnet–orthopyroxene and orthopyroxene–clinopyroxene relationships in simple and complex systems. *Contr. Miner. Petrol.*, **42**, 109–124.

*Received 2 January 1985; revision accepted 8 March 1985.*